The Promise of Low Dimensional Systems for Thermoelectric Applications

M. S. Dresselhaus

Massachusetts Institute of Technology

Group members

Yu-Ming Lin,
Steve B. Cronin,
Marcie R. Black,
Oded Rabin
Dr. Gene Dresselhaus

Collaborators

Dr. Jos Heremans, Dr. Ted Harman
Prof. Rogacheva, Prof. Jackie Y. Ying,
Prof. Gang Chen

Motivation

Seebeck Coefficient

Conductivity

Temperature

$$ZT = \frac{S^2 \sigma T}{\kappa}$$

Thermal Conductivity

$ZT \sim 3$ for desired goal

Difficulties in increasing ZT in bulk materials:

$S \uparrow \Longleftrightarrow \sigma \downarrow$

$\sigma \uparrow \Longleftrightarrow S \downarrow$ and $\kappa \uparrow$

$\Rightarrow$ A limit to Z is rapidly obtained in conventional materials

$\Rightarrow$ So far, best bulk material ($Bi_{0.5}Sb_{1.5}Te_3$) has $ZT \sim 1$ at 300 K

Low dimensions give additional control:

- Enhanced density of states due to quantum confinement effects
  - $\Rightarrow$ Increase S without reducing σ
- Boundary scattering at interfaces reduces κ more than σ
- Possibility of carrier pocket engineering to further improve ZT

Enhanced Thermoelectric Properties of Conventional Materials

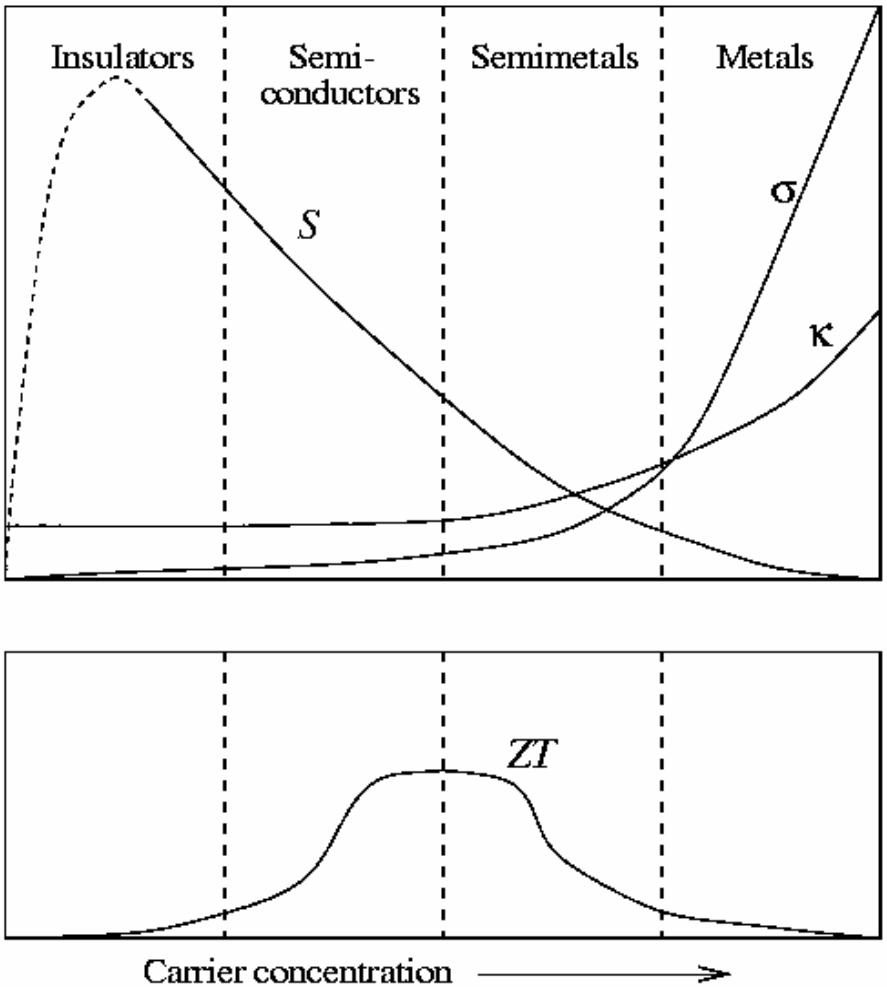

To increase Z, we want

$$S\uparrow,\quad \sigma\uparrow,\quad \kappa\downarrow$$

but

$$S\uparrow \Leftrightarrow \sigma\downarrow$$

$$\sigma\uparrow \Leftrightarrow \kappa\uparrow$$

With known conventional solids, a limit to Z is rapidly obtained.

Best alloy: $Bi_{0.5}Sb_{1.5}Te_3$

$ZT \sim 1$ @ 300 K

Introduction to Low Dimensions

- Density of states and predicted *ZT*:

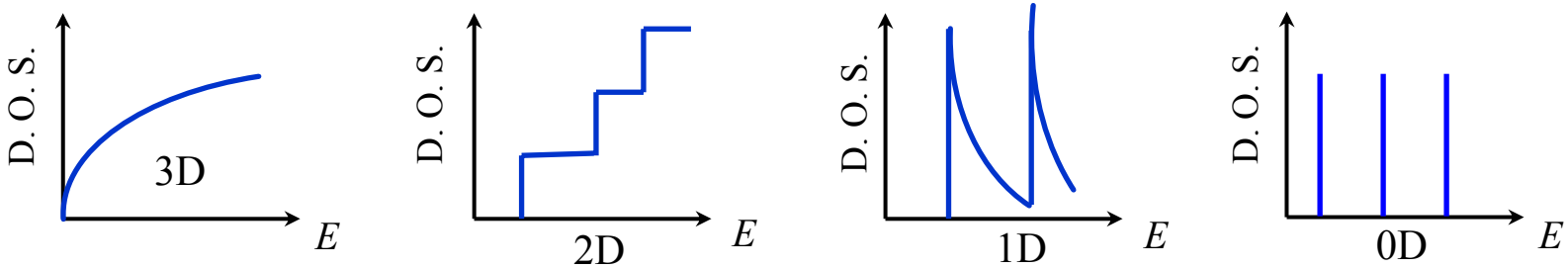

- Promising low-dimensional systems:
  - 2D Quantum Wells: $PbTe/PbEu_{1-x}Te_x$
    Si/Ge and GaAs/AlAs
  - 1D Quantum Wires: Bi and $Bi_{1-x}Sb_x$
  - 0D Quantum Dots: $PbSe_xTe_{1-x}$
    segmented nanowires

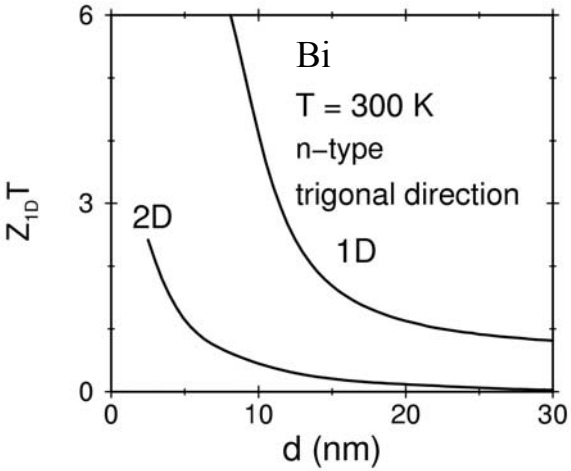

Low Dimensional Enhancement

Proof of Principle 2D

$$ZT = \frac{(S^2 n) e \mu}{\kappa} T$$

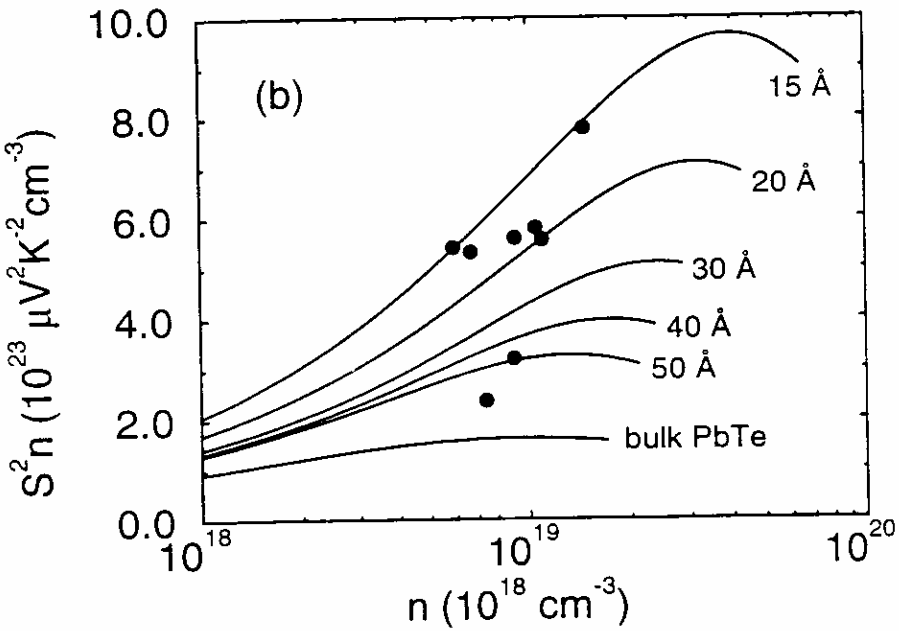

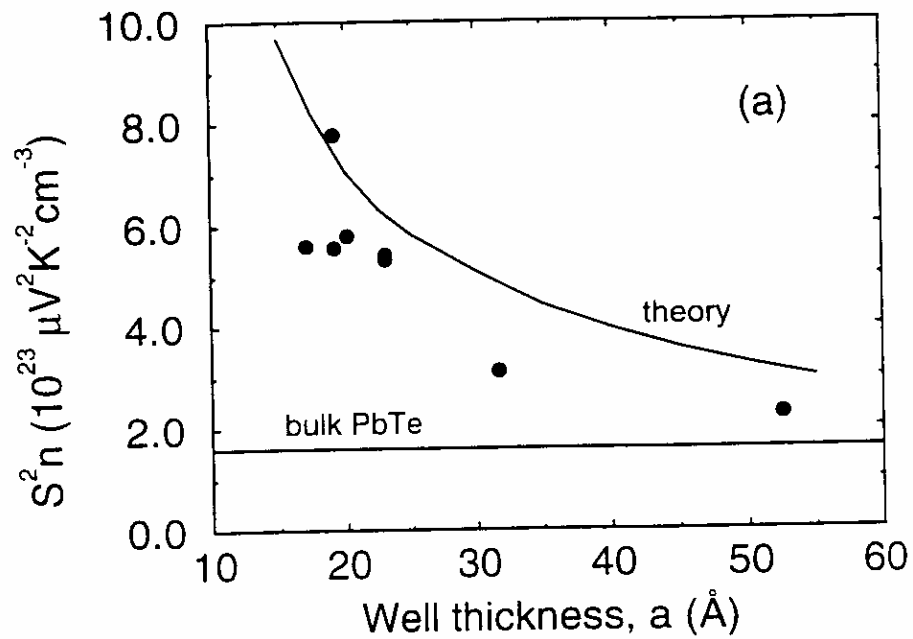

$PbTe/Pb_{0.927}Eu_{0.073}Te$ superlattice samples with thick barrier layers show enhanced thermoelectric properties relative to bulk values for small quantum well widths (1996).

Carrier Pocket Engineering Approach to Enhance $Z_{3D}T$

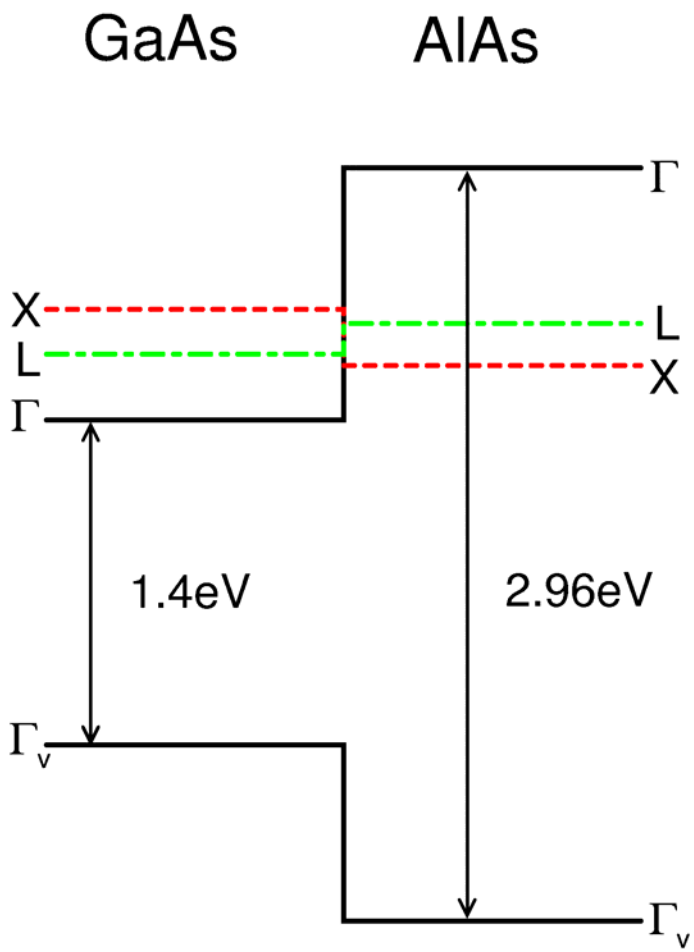

Application of Carrier Pocket Engineering Concept in GaAs/AlAs quantum well superlattice systems

- Optimization of well and barrier widths
- Determination of lattice growth orientation
- Enhancement in *ZT* from various carrier pockets other than Γ point pockets

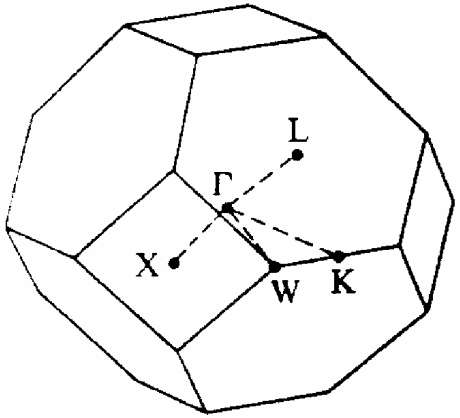

- Concept successfully applied to GaAs/AlAs and $Si/Si_{1-x}Ge_x$ superlattices.

Enhanced *ZT* in $PbSe_xTe_{1-x}$/PbTe Quantum Dot Superlattices

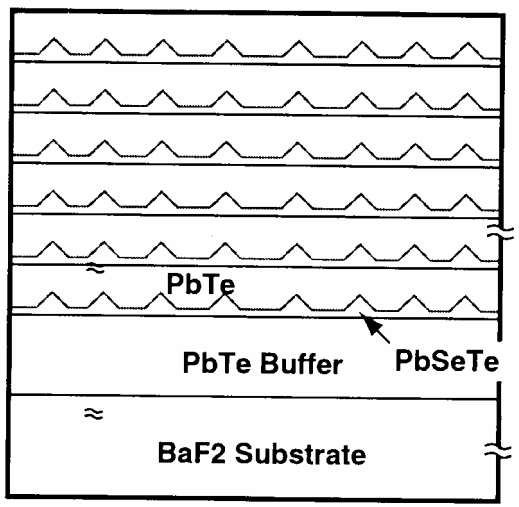

$PbSe_xTe_{1-x}$ quantum dots in PbTe layers

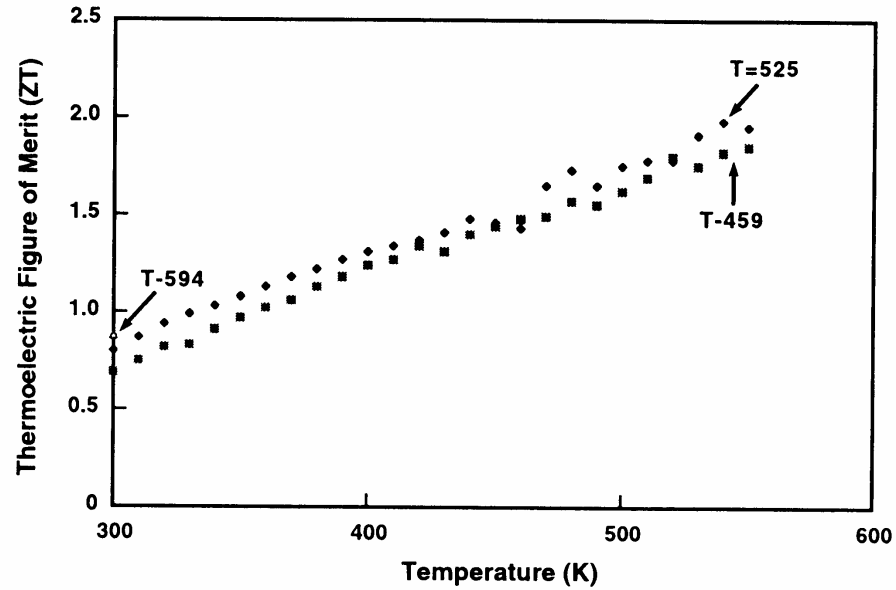

Harman et al. J. Electron. mater. Lett. ***29****, L1 (2000)*

- Enhancement of *ZT* at 300 K in quantum dot superlattice is more than a factor of two relative to best available bulk PbTe
  - More favorable carrier scattering mechanism due to adsorbed or precipitated Te
  - Partial carrier confinement in quantum dots of $PbSe_{0.98}Te_{0.02}$
  - Lower lattice thermal conductivity in alloy
- Highest $ZT = 2$ is obtained in quantum dot superlattice

Thermoelectrics in 1D systems — Bi nanowires

- Why Bi ?
  - Smallest electron effective mass (~$0.001m_0$) of known materials.

    ⇒ Favorable to observe quantum confinement effects
  - Highly anisotropic Fermi surface (ratio > 100)

    ⇒ More variability for band structures
  - Long mean free path (~mm at 4 K)

    ⇒ Suitable for studying transport properties
  - Low carrier concentration (~$10^{18}cm^{-3}$)

    ⇒ Can be easily managed by doping: Te (*n*-type) or Pb, Sn (*p*-type)

Band Structure of Bi

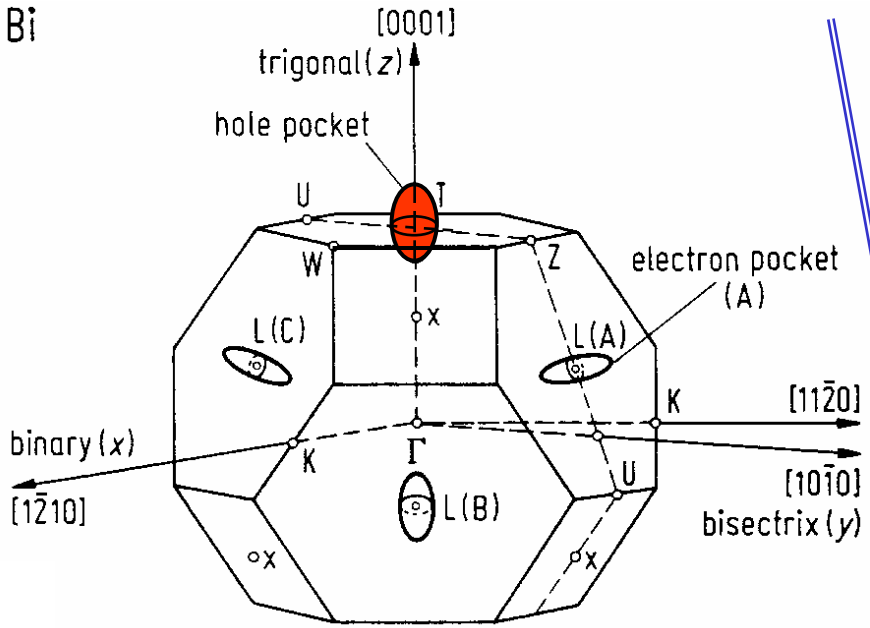

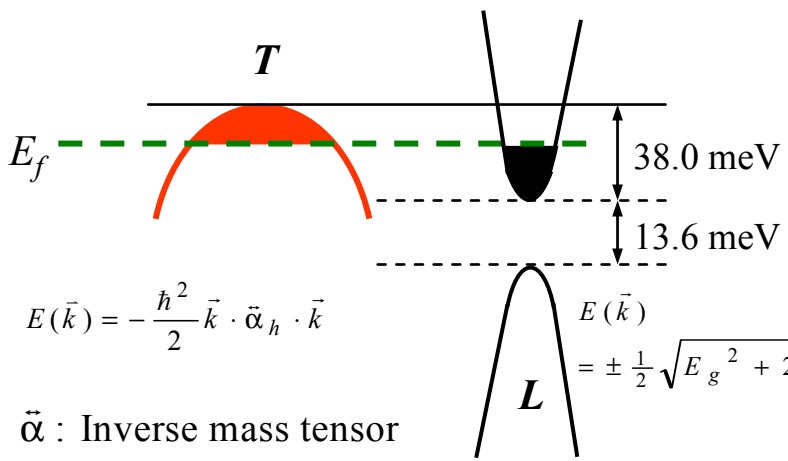

$$E(\vec{k}) = -\frac{\hbar^2}{2}\vec{k}\cdot\overleftrightarrow{\alpha}_h\cdot\vec{k}$$

$$E(\vec{k}) = \pm\frac{1}{2}\sqrt{E_g^{\,2} + 2E_g\hbar^2\vec{k}\cdot\overleftrightarrow{\alpha}_e\cdot\vec{k}}$$

$\overleftrightarrow{\alpha}$: Inverse mass tensor

Effective Mass Tensors:

L-point Electron Pocket(A) :

$$\overleftrightarrow{M}_A^e = \begin{pmatrix} m_{e1} & 0 & 0 \\ 0 & m_{e2} & m_{e4} \\ 0 & m_{e4} & m_{e3} \end{pmatrix}$$

$$m_{e1} = 0.00119m_0, m_{e2} = 0.263m_0$$

$$m_{e3} = 0.00516m_0, m_{e4} = 0.0274m_0$$

T-point Hole Pocket:

$$\overleftrightarrow{M}_h = \begin{pmatrix} m_{h1} & 0 & 0 \\ 0 & m_{h1} & 0 \\ 0 & 0 & m_{h3} \end{pmatrix}$$

$$m_{h1} = 0.059m_0$$

$$m_{h3} = 0.634m_0$$

Template-Assisted Nanowire Fabrication

- Synthesis of porous templates (e.g., anodic alumina)
- Filling of nanopores with target material
  - Pressure injection
  - Vapor deposition
  - Electrochemical deposition
- Post-filling treatment

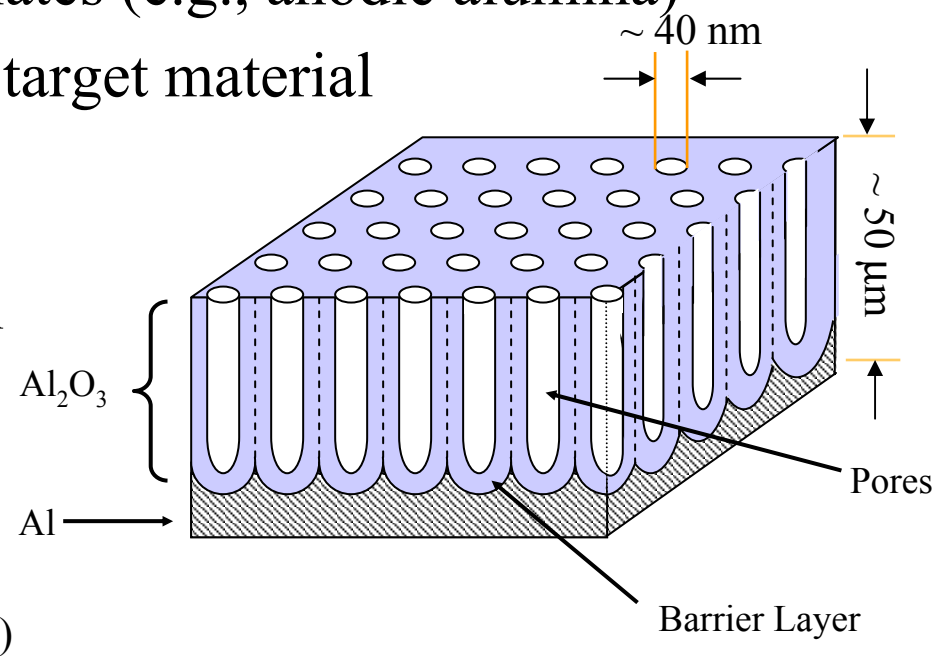

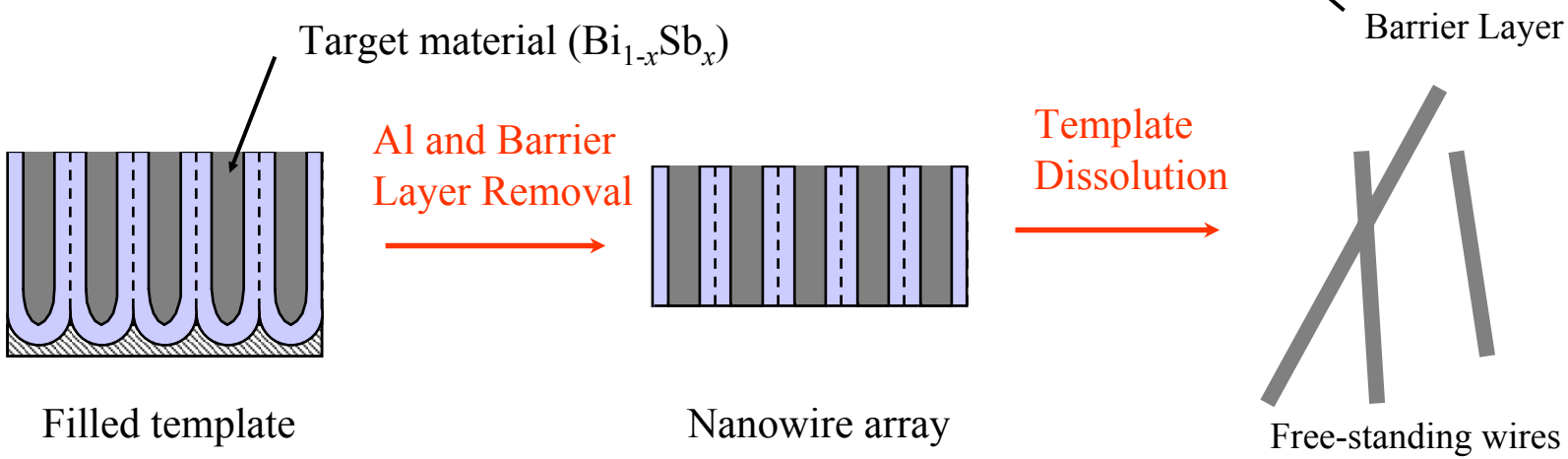

Synthesis of Nanowires

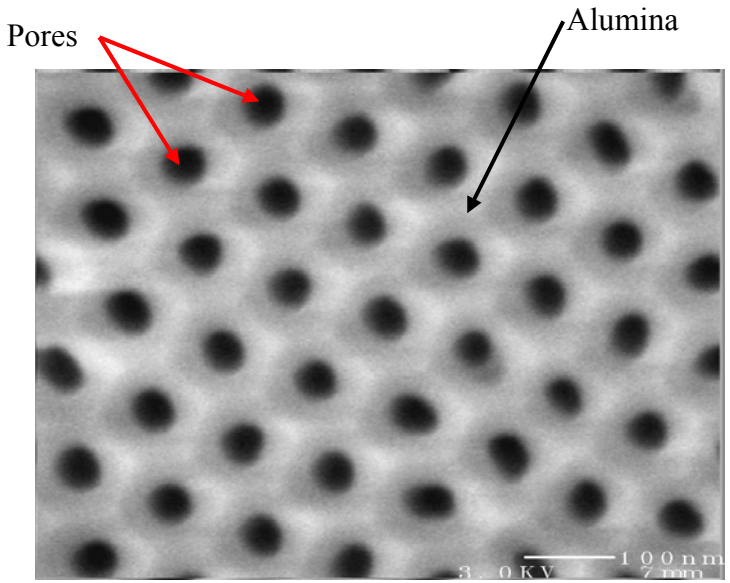

SEM image of top surface of porous alumina anodized in 4 wt% $H_2C_2O_4$ at 45 V. The pore diameter is ~ **44** nm.

Pressure Injection

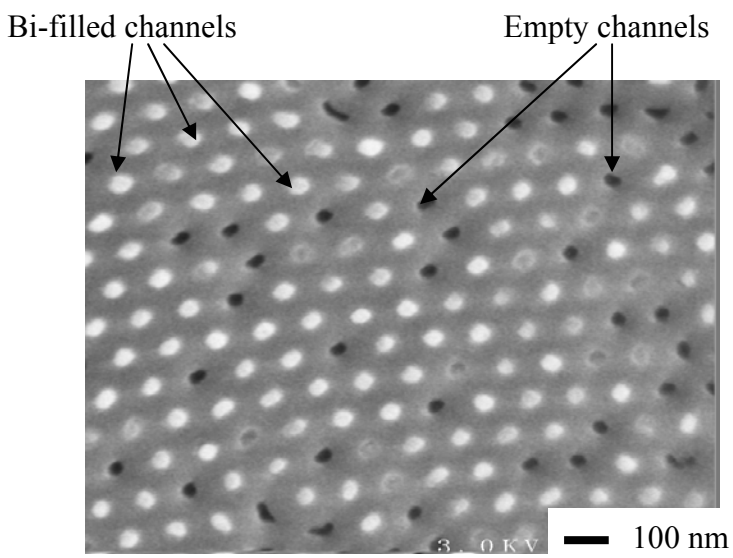

SEM image of bottom surface of Bi nanowire arrays after the barrier layer has been removed. The wire diameter is ~ **40** nm.

X-Ray Diffraction of Nanowire Arrays

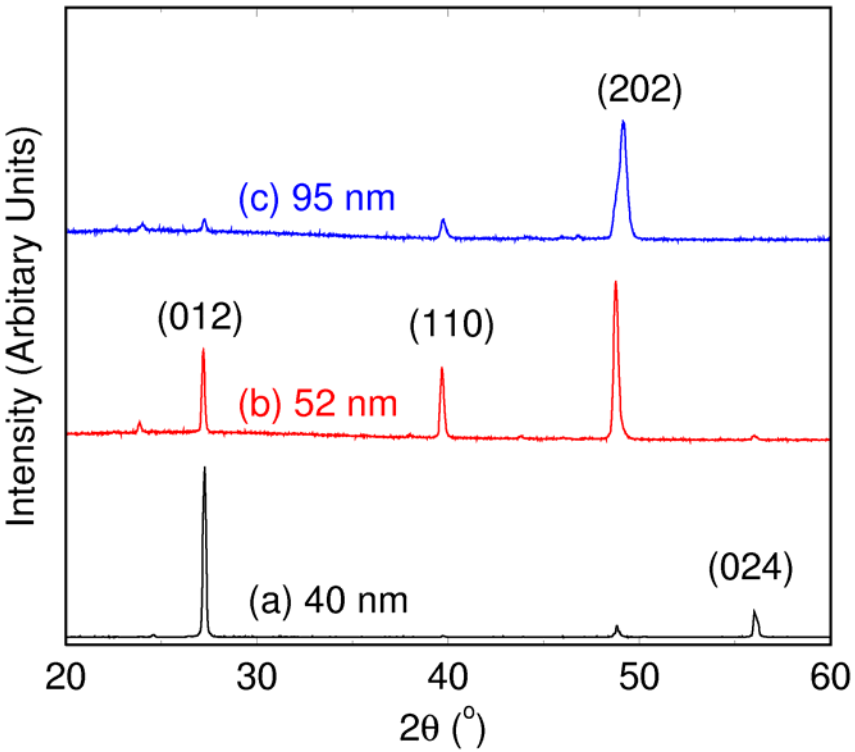

X-ray diffraction of Bi nanowire arrays with different diameters: (a) 40 nm, (b) 52 nm, and (c) 95 nm.

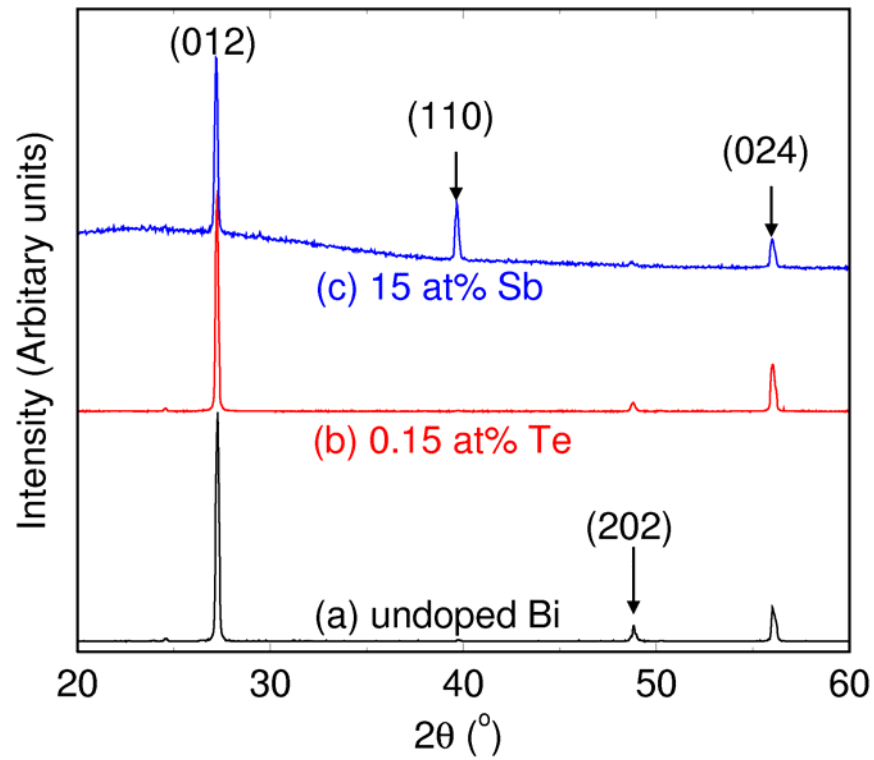

X-ray diffraction of 40-nm Bi nanowire arrays with different compositions: (a) undoped, (b) doped with 0.15 at% Te, and (c) alloyed with 15 at% Sb.

TEM and Electron Diffraction

- The nanowires are uniform, continuous and highly crystalline

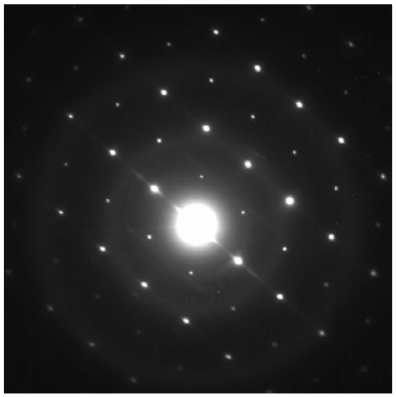

Electron diffraction

High resolution TEM of a 40-nm Bi nanowire

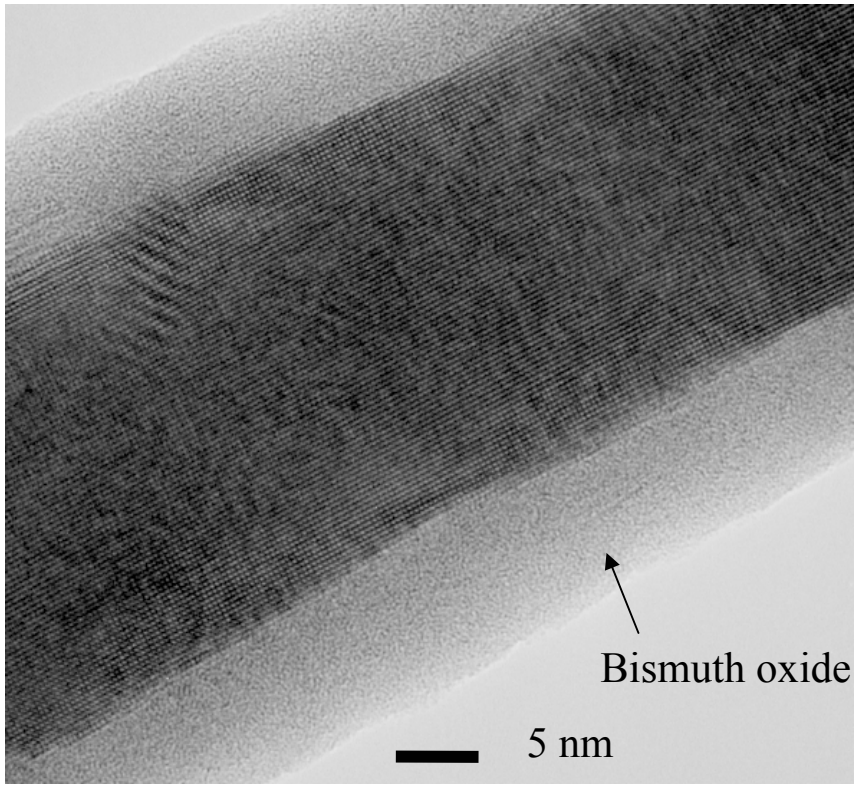

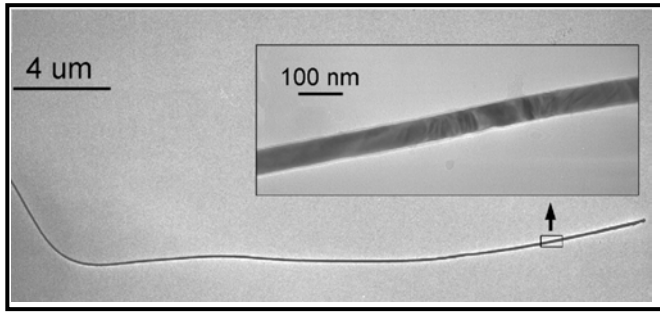

TEM image of a long free-standing Bi nanowire . The average wire diameter is ~ **65** nm.

Semimetal-Semiconductor Transition in Bi

- Bi
  - Group V element
  - Semimetal in bulk form
  - The conduction band (*L*-electron) overlaps with the valence band (*T*-hole) by 38 meV

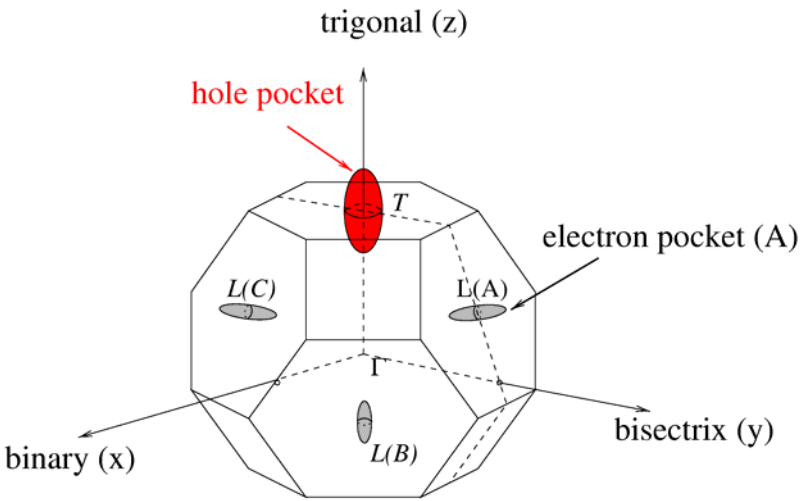

Brillouin zone of Bi

- Bi nanowire
  - Semimetal-semiconductor transition at a wire diameter about 50 nm due to quantum confinement effects

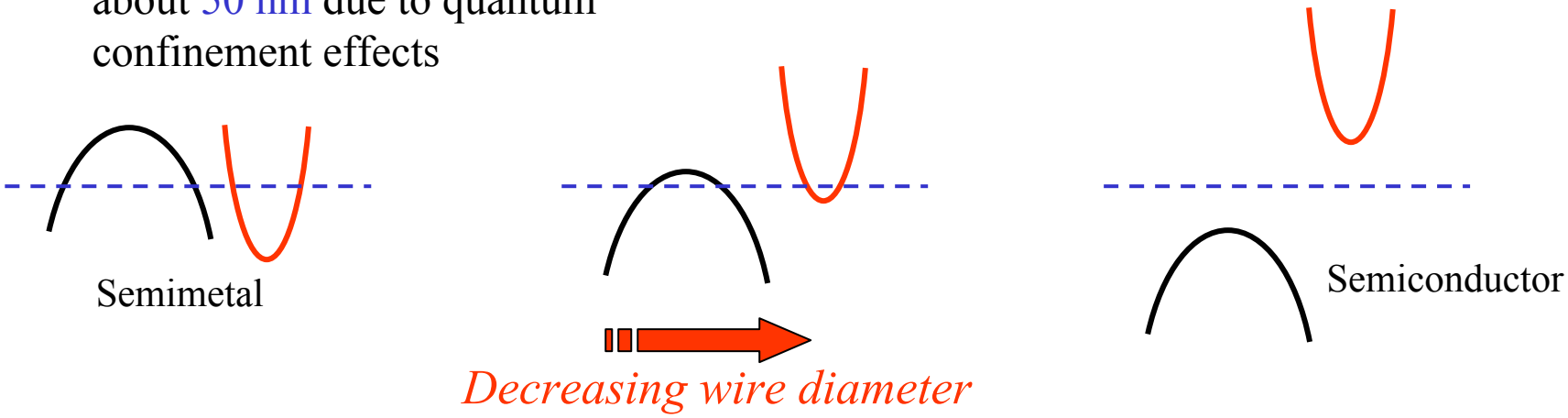

Measured $R(T)$ of Bi Nanowire Arrays

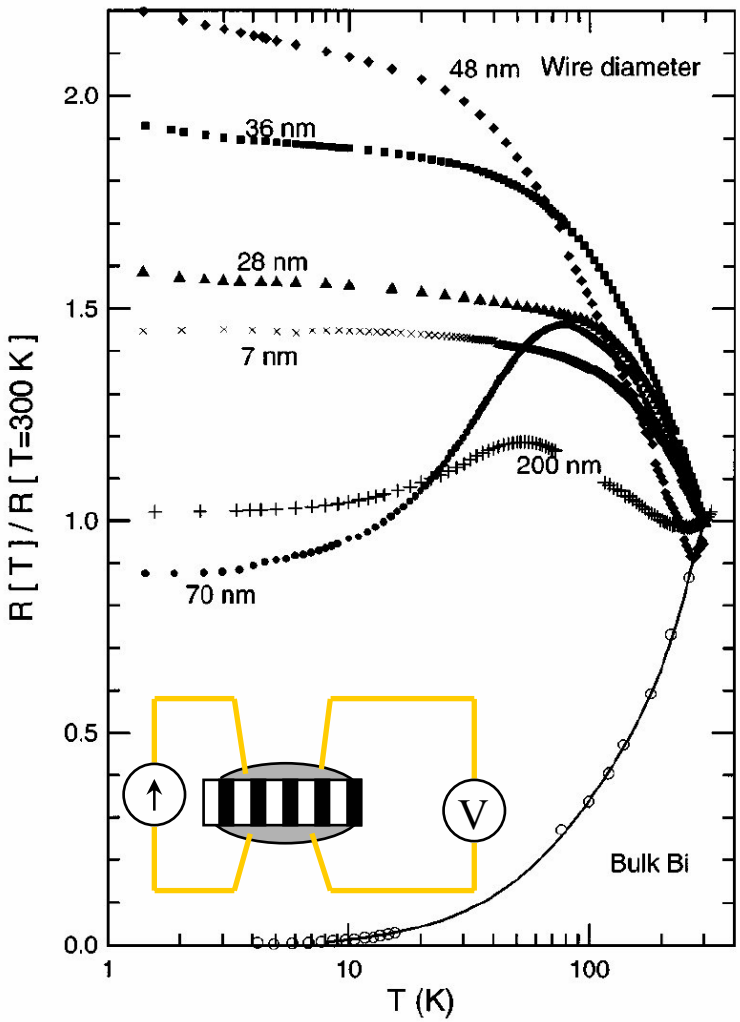

Theoretical Modeling:

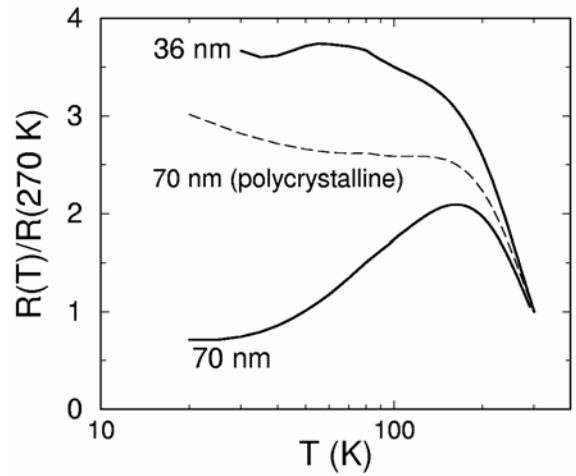

- Uncontrolled impurity
- Matthiessen's rule:

$$\frac{1}{\mu_{tot}} = \frac{1}{\mu_{bulk}} + \frac{1}{\mu_{boundary}} + \frac{1}{\mu_{imp}}$$

Measured $R(T)$ for different wire diameters.
[J. Heremans *et al*]

- Provides confirmation of modeling
- Provides evidence for semimetal-semiconductor transition

Boundary Scattering Effect

Magnetoresistance

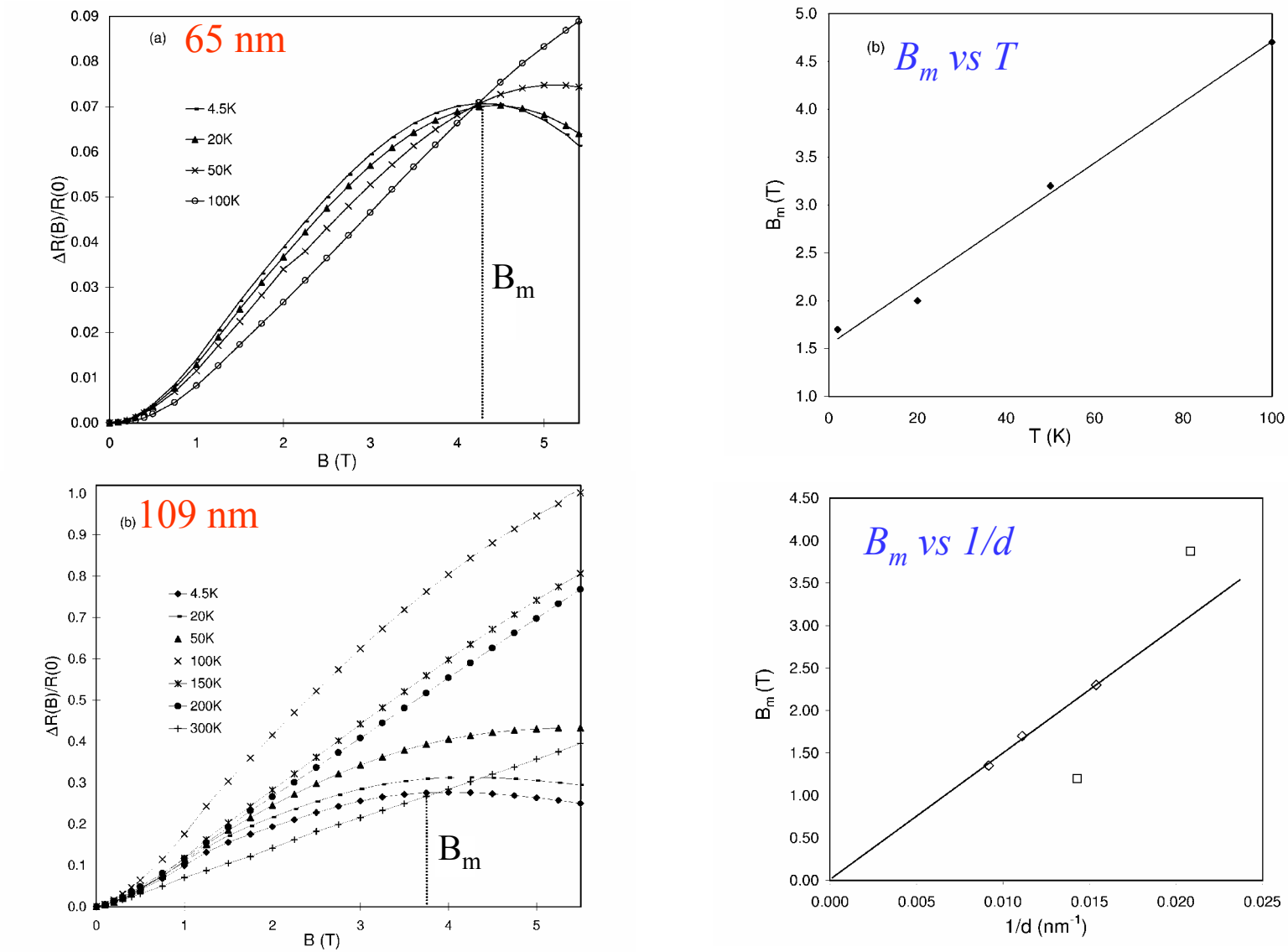

- Provides evidence for wire boundary scattering and for ballistic transport

Seebeck Coefficient Measurements

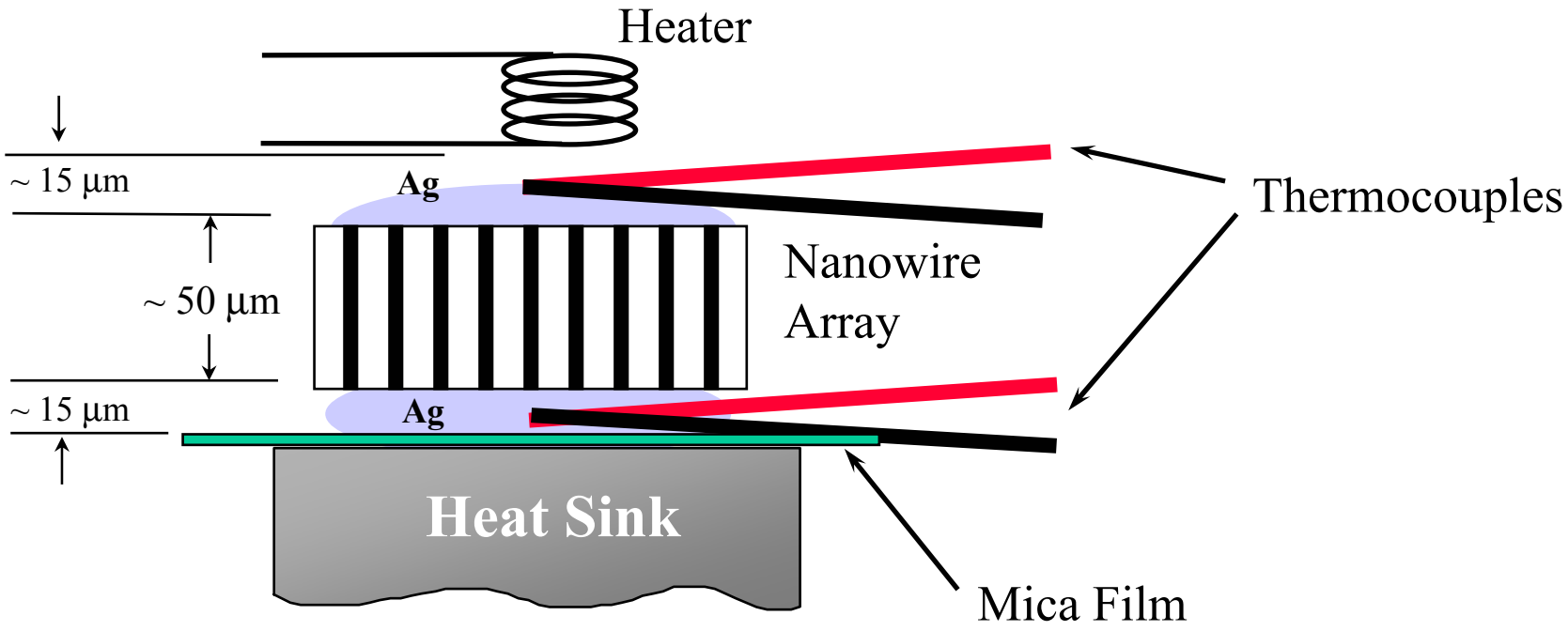

Seebeck Coefficient of 200 nm Bi Nanowires

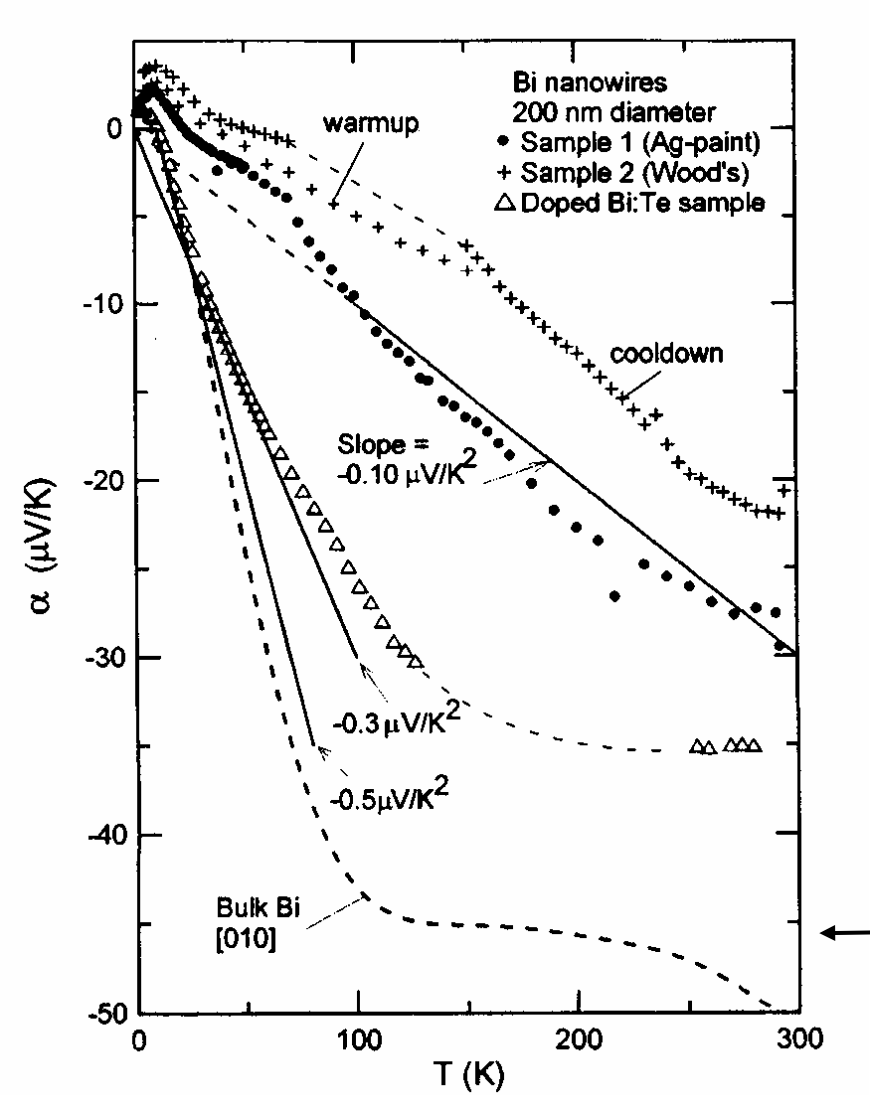

Theoretical Model of 120 nm Bi nanowires

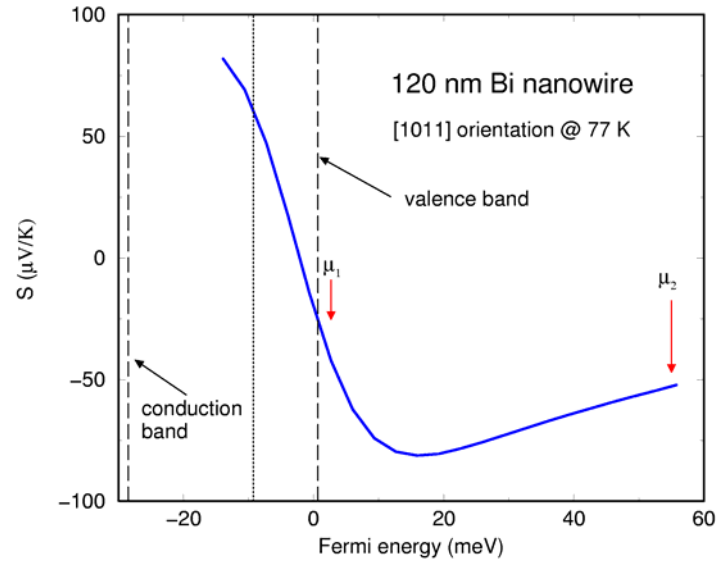

- For semimetallic Bi nanowires, the thermoelectric power increases with Te dopant concentration.

Seebeck measurements of 200 nm Bi nanowire arrays as a function of *T*.

J. Heremans et. al., Phys. Rev. B ***59****, 12579 (1999)*

Measurements of Individual Bi Nanowires

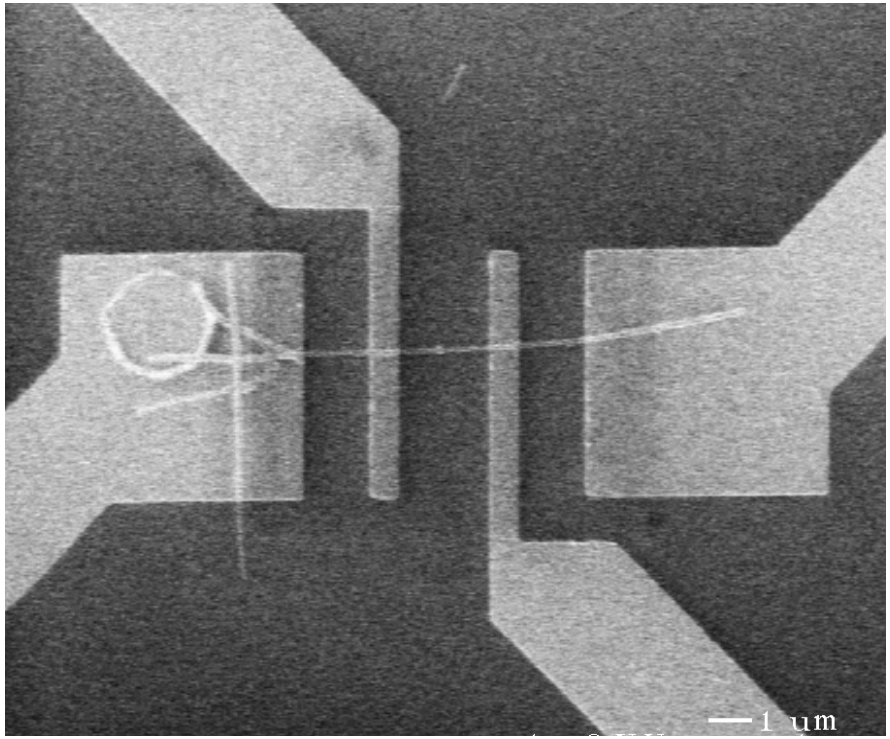

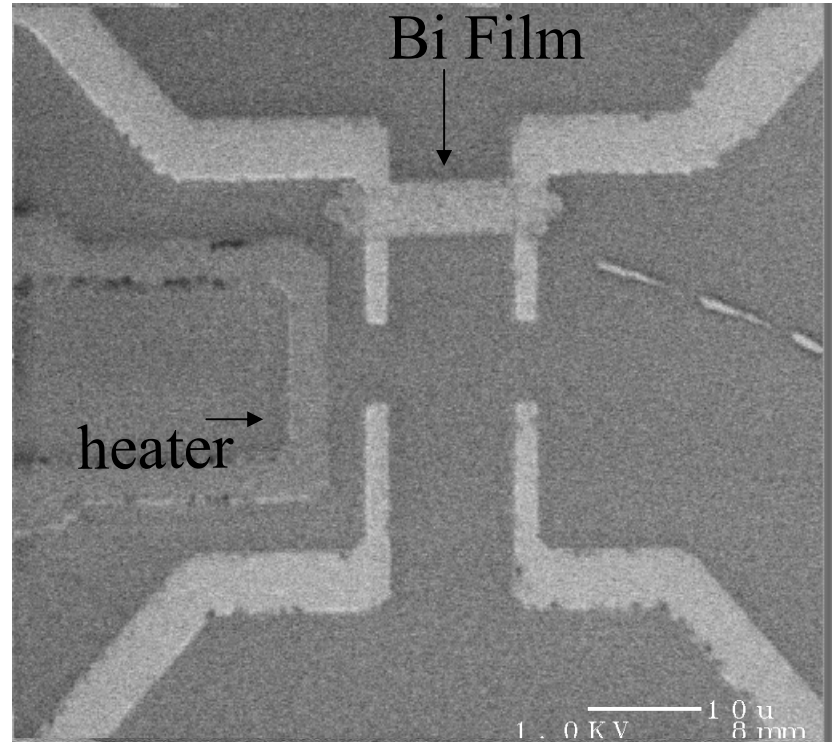

4-Point Resistivity Measurement

- Contact resistance > 1MΩ
- Non-linear I-V

Differential Seebeck Measurement

- Seebeck measured with respect to known bulk Bi film

$$S = \frac{\Delta V}{\Delta T}$$

- ΔT~0.5K easily attained

4-Point Measurement at Room Temperature of a 200nm Bi nanowire

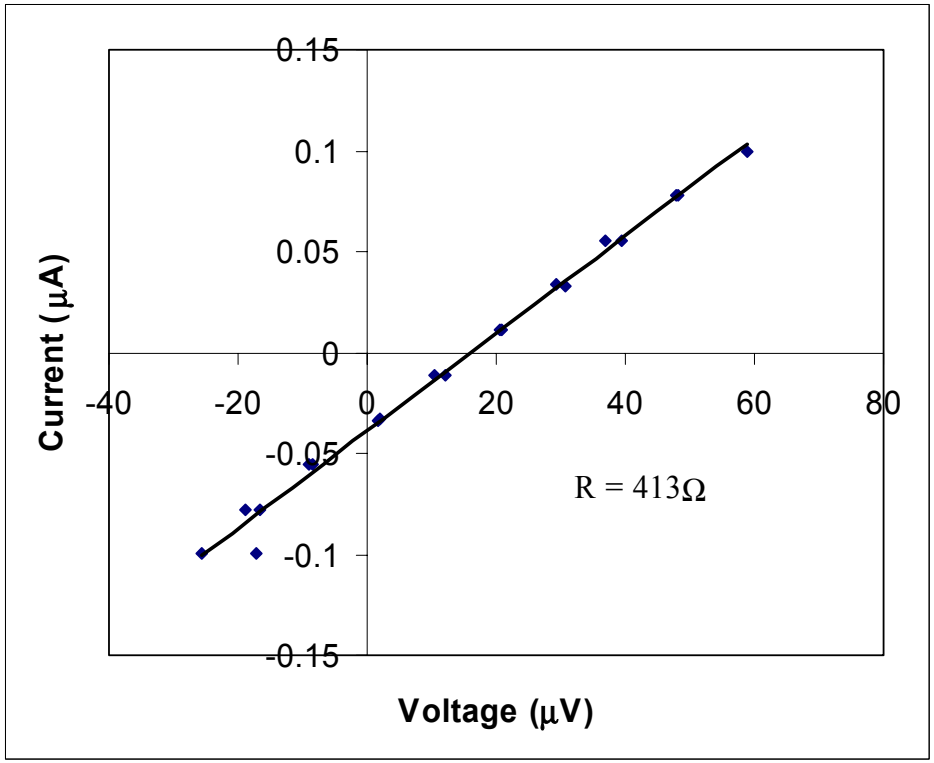

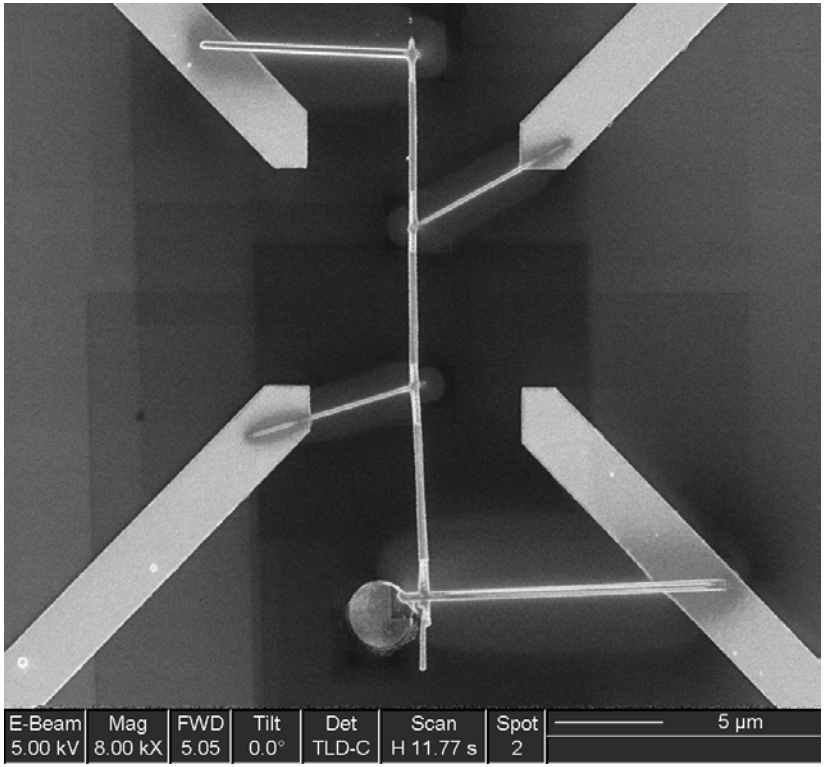

Diameter = 200nm
Length = 6.9μm
$R_{sample} = 413\Omega$
$R_{contacts} = 4k\Omega$
T=300K

$$\rho_{sample} = \frac{R \cdot A}{L} = 1.88 \times 10^{-4}\,\Omega \cdot cm \approx \rho_{bulk}$$

$$\rho_{bulk} = 1.2 \times 10^{-4}\,\Omega \cdot cm$$

Optical Properties Measurements

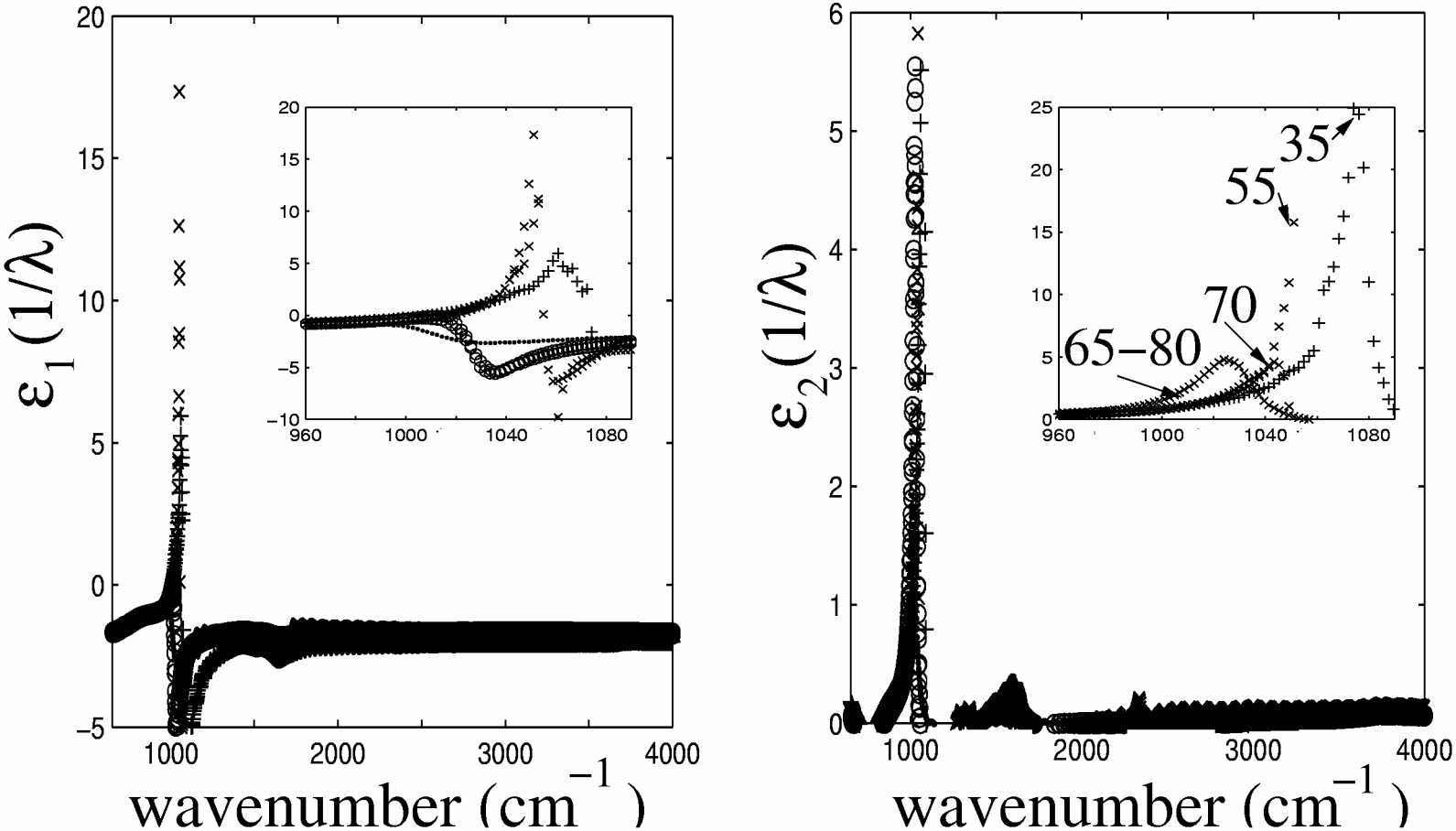

The dielectric function ($\varepsilon_1 + i\varepsilon_2$) of Bi nanowires with different diameters obtained from analysis of reflectivity measurements.

Alumina Templates on Silicon Wafers

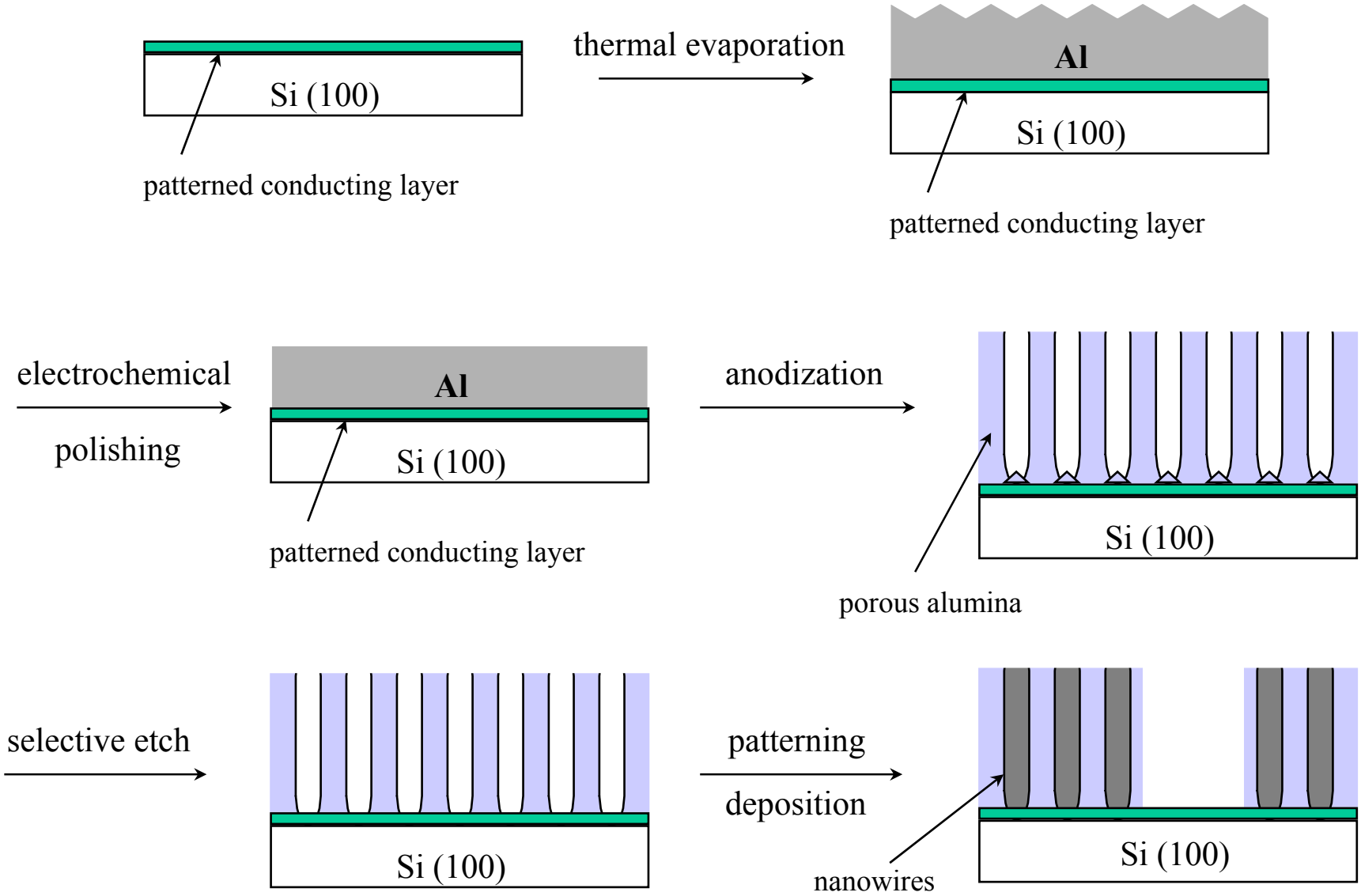

Nanowire Growth in Templates

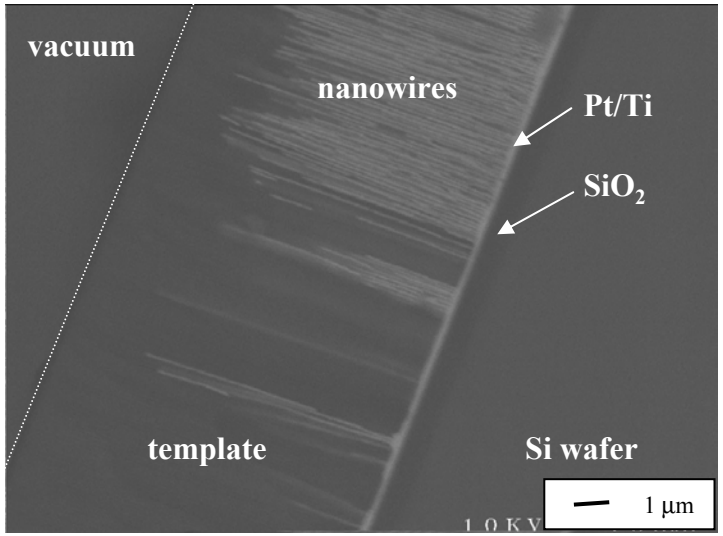

Bismuth nanowires grown by electrochemical deposition (composition-contrast image).

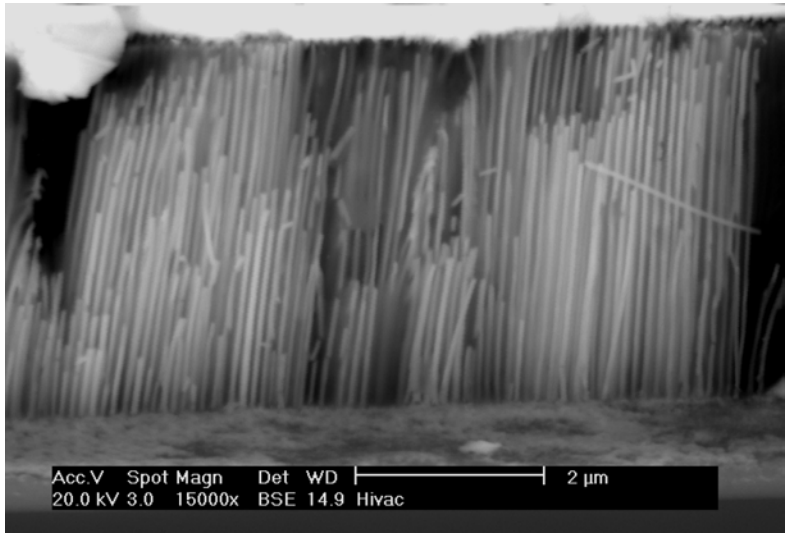

Bi_2Te_3 nanowires grown by electrochemical deposition (courtesy of Dr. M. A. Ryan).

Towards Multi-Component Nanowire Arrays

By means of lithography, a design allowing deposition of both *p*-type and *n*-type components on the same support could be achieved.

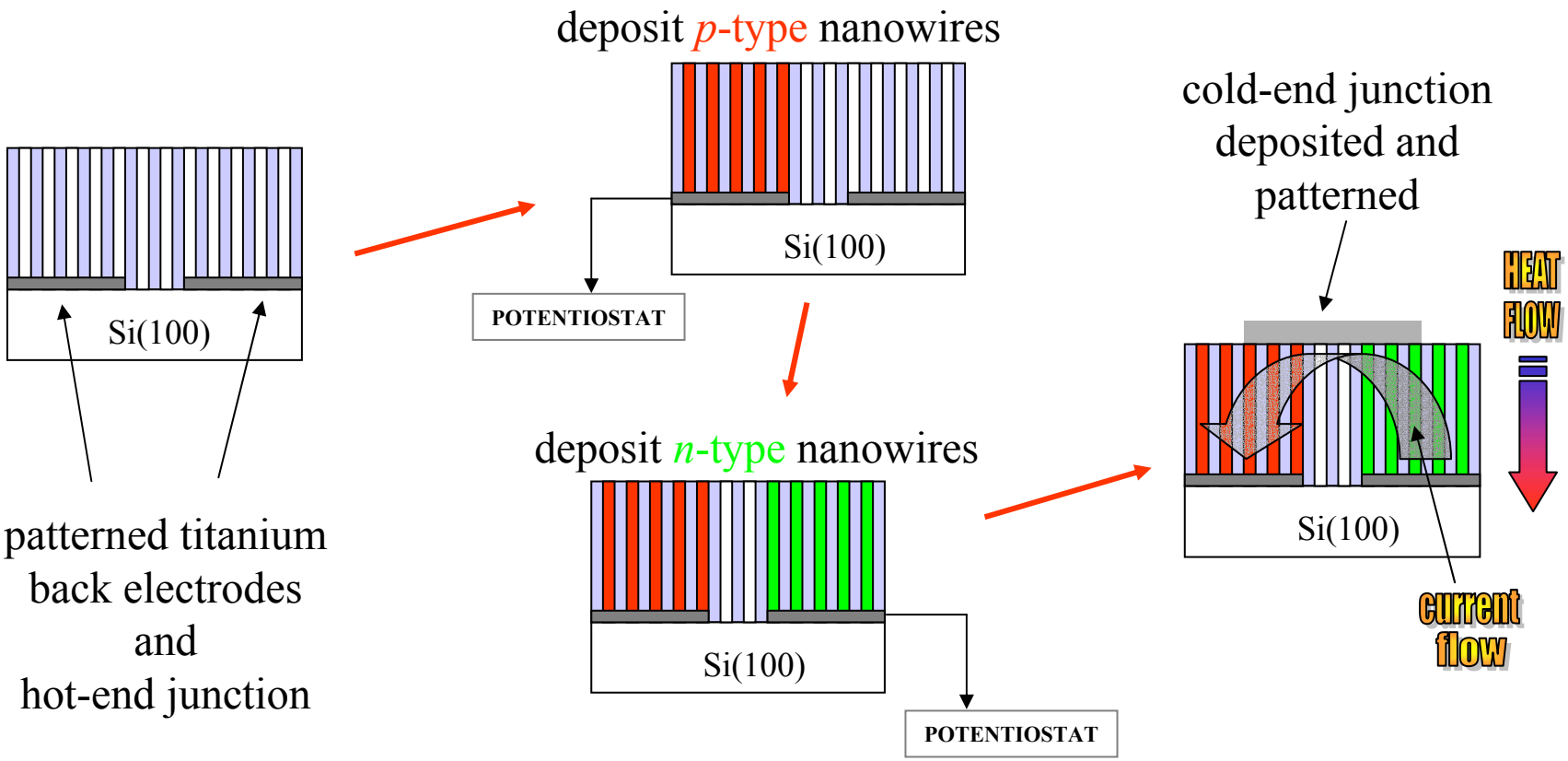

$Z_{1D}T$ of n-type Bi Nanowires

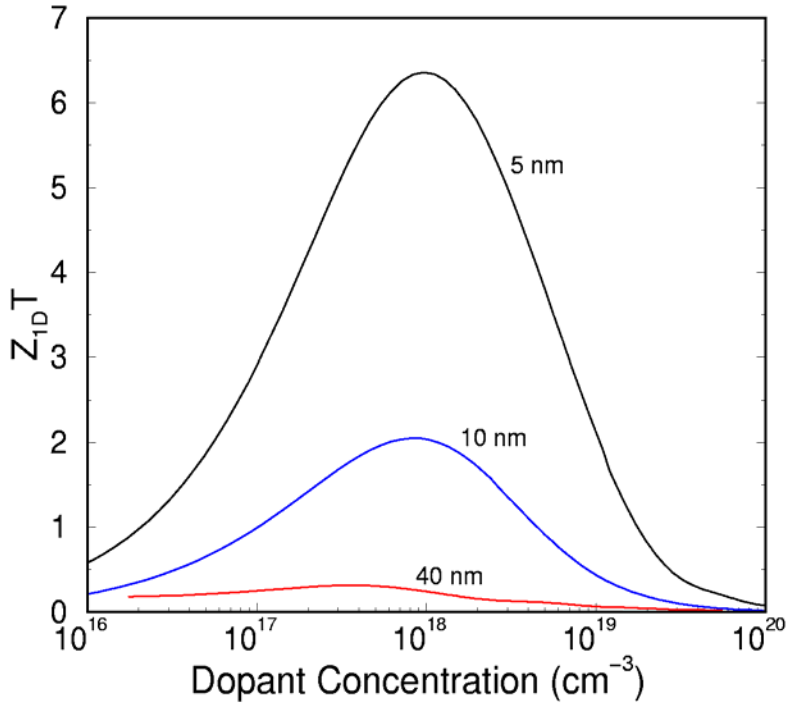

$Z_{1D}T$ as a function of donor concentration for different wire diameters at 77 K. Wire orientation: Trigonal.

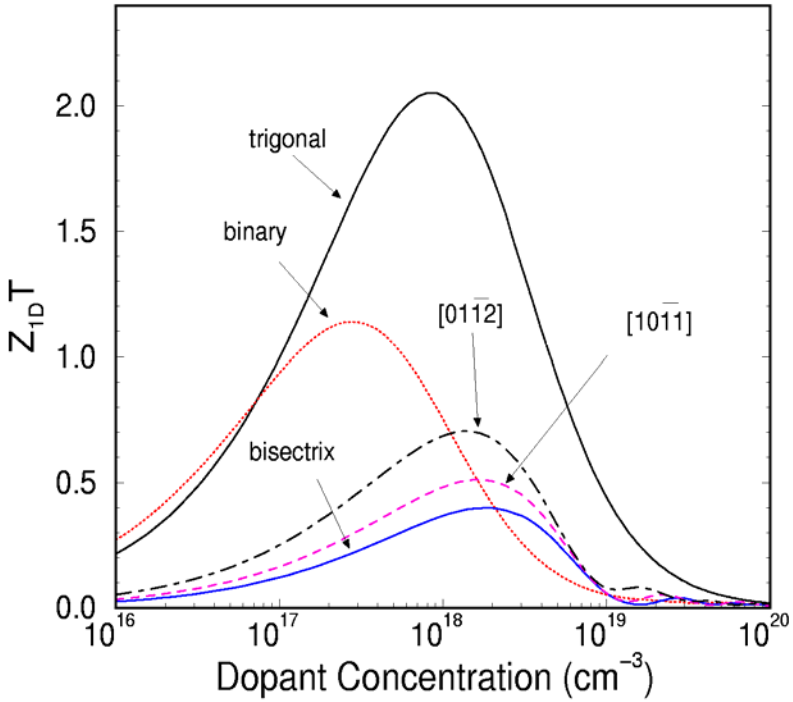

$Z_{1D}T$ as a function of donor concentration for different wire orientations. (77 K) Wire diameter: 10 nm.

Optimal $Z_{1D}T$: Trigonal > Binary > (012) > (101) > Bisectrix

Carrier Pocket Engineering — $Bi_{1-x}Sb_x$ Alloy

- Bi and Sb
  - Group V elements
  - Semimetals in bulk form
  - Completely miscible with each other
  - Introduction of Sb in Bi moves down the *T*-point valence band edge in energy relative to the *L*-point carriers
  - Provides a promising approach to achieve desirable band structure (i.e., semiconducting) in Bi nanowires

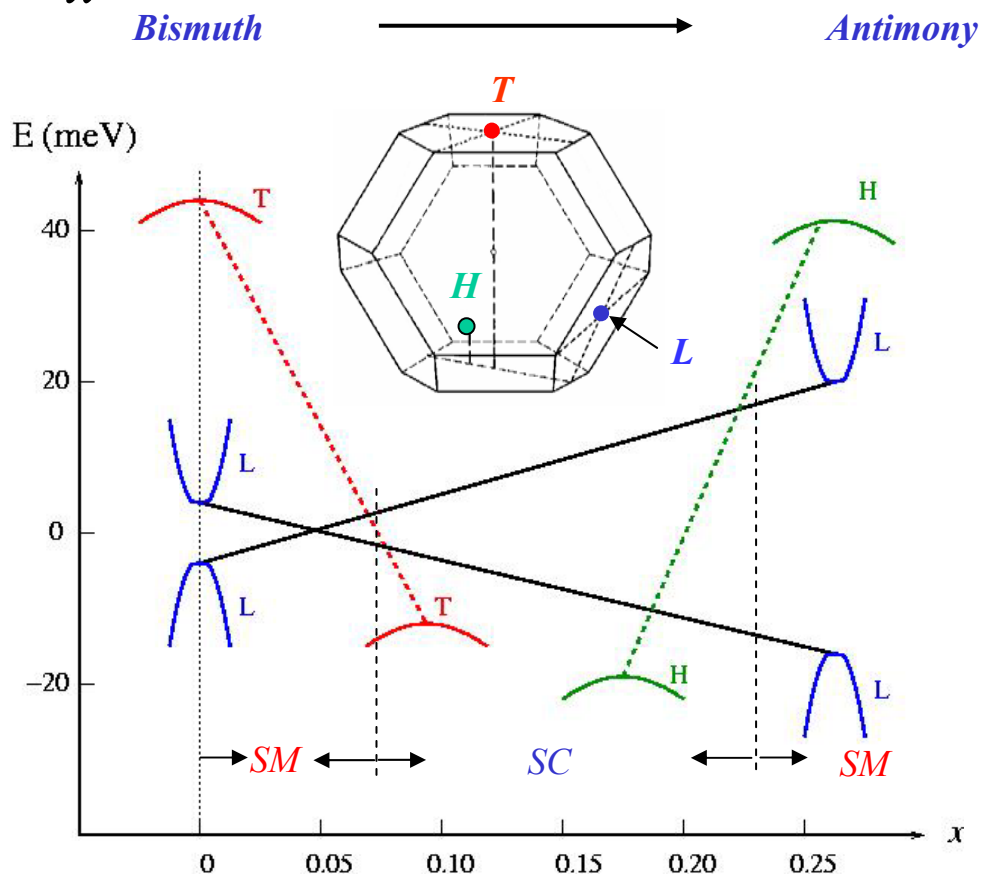

Band structure of $Bi_{1-x}Sb_x$ alloy as a function of Sb concentration x.

SM: Semimetal
SC: Semiconductor

Electronic Band Structure of $Bi_{1-x}Sb_x$ Nanowires

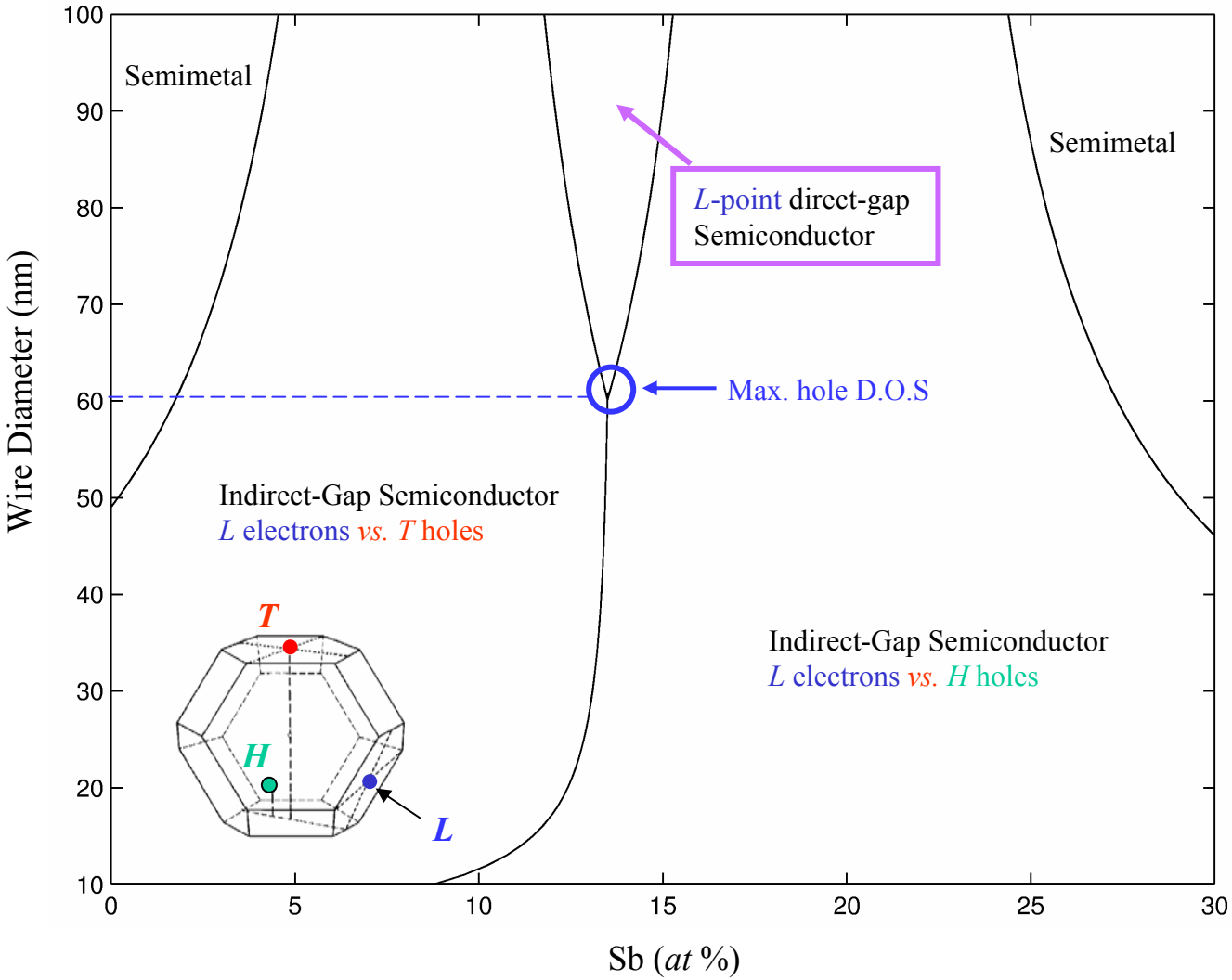

Predicted $Z_{1D}T$ of $Bi_{1-x}Sb_x$ Nanowires

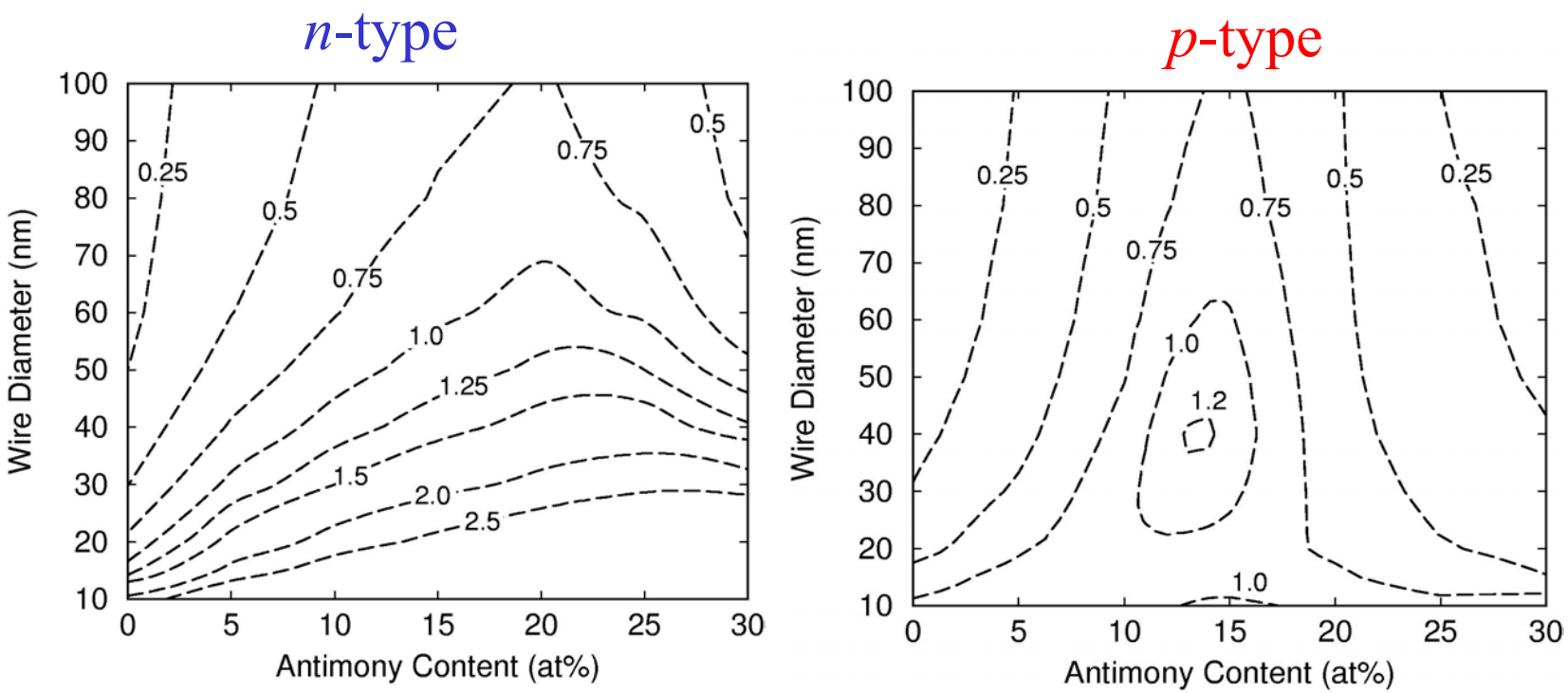

- $Z_{1D}T$ of both *p*-type and *n*-type $Bi_{1-x}Sb_x$ nanowires are improved, and performance of practical interest is predicted at easily accessible wire diameters
- *n*-type and *p*-type nanowires have matched *ZT* (~1.2) at a wire diameter of ~ 40 nm and Sb concentrations of $x \sim 0.13$

Semimetal-Semiconductor Transition

Observation

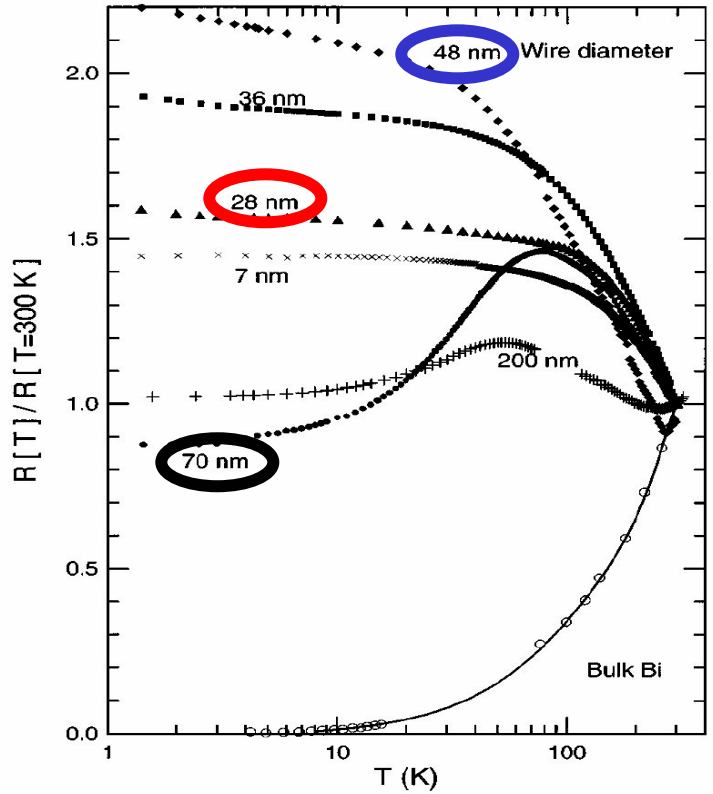

Measured $R(T)$ of pure Bi nanowires.
J. P. Heremans et al.

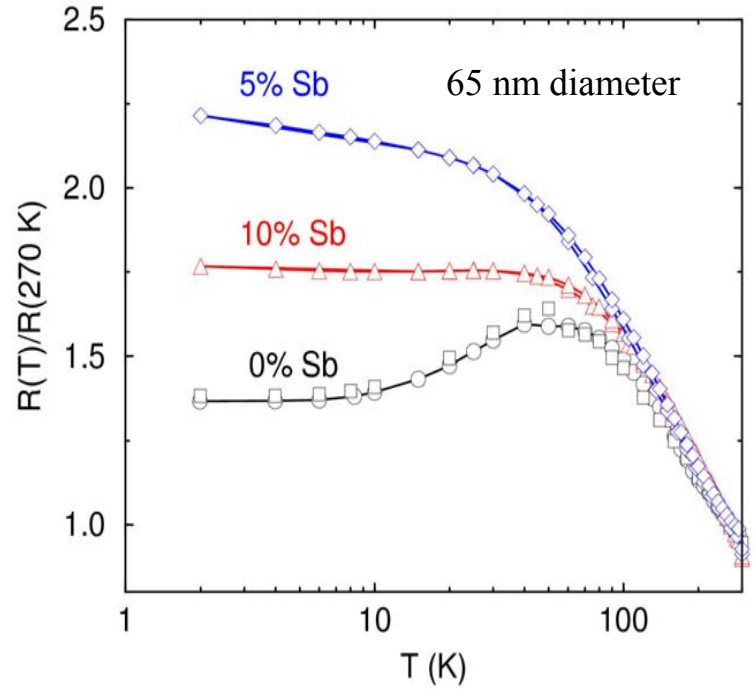

Measured $R(T)$ of 65-nm $Bi_{1-x}Sb_x$ nanowires.

65-nm $Bi_{1-x}Sb_x$ nanowires exhibit semimetal-semiconductor transition behaviors similar to those of pure Bi nanowires.

Seebeck Coefficient Measurements

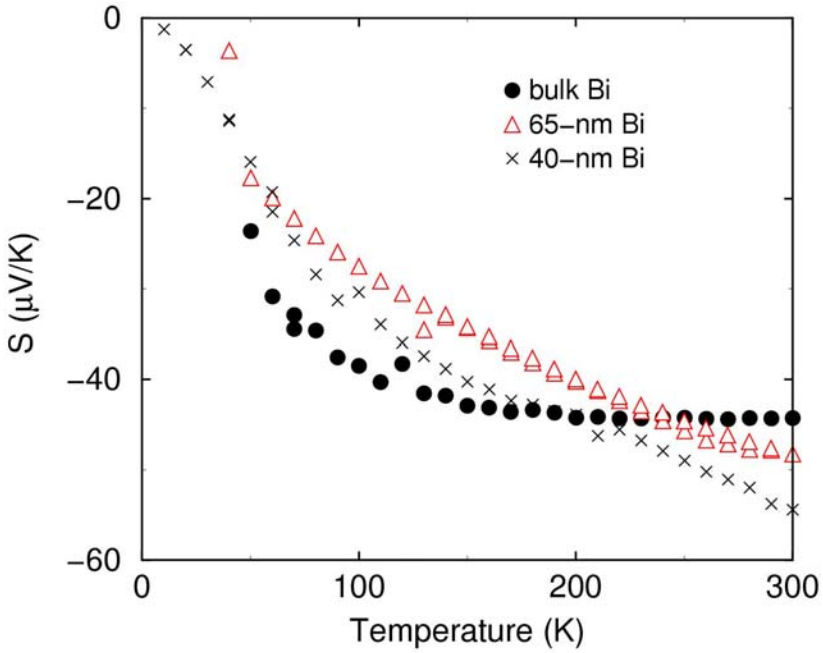

Measured Seebeck coefficient as a function of temperature for 40-nm and 65-nm Bi nanowire arrays

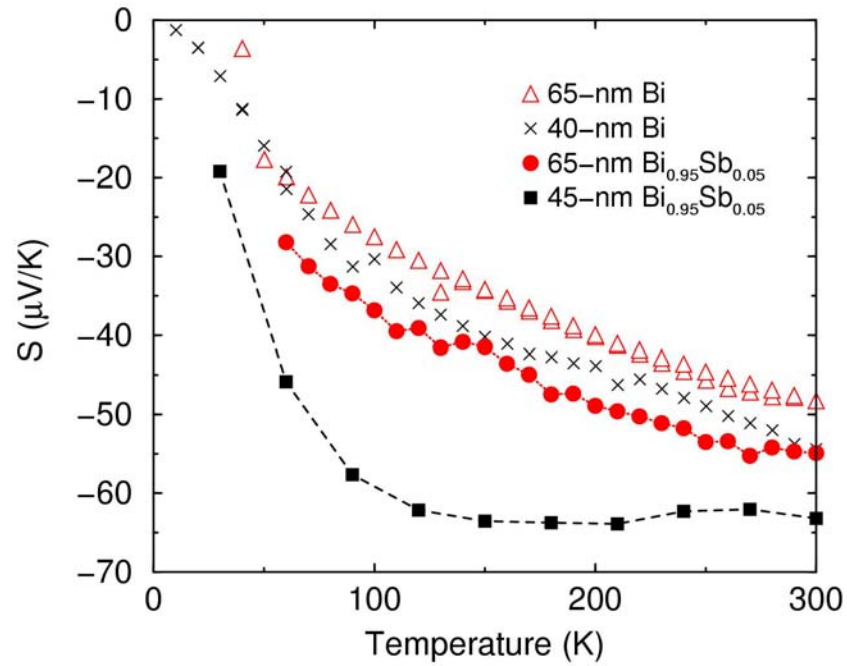

Measured Seebeck coefficient as a function of temperature for 40-nm and 65-nm Bi and $Bi_{0.95}Sb_{0.05}$ nanowire arrays

*Bulk Bi is taken from excess Bi pieces after the pressure injection

Thermoelectrics in Low-D Systems

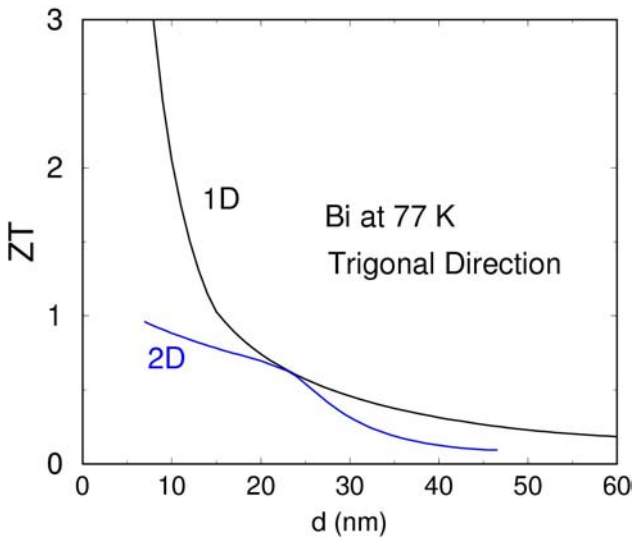

Superlattice (2D)

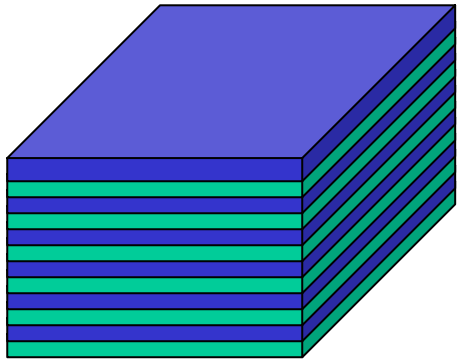

Nanowire (1D)

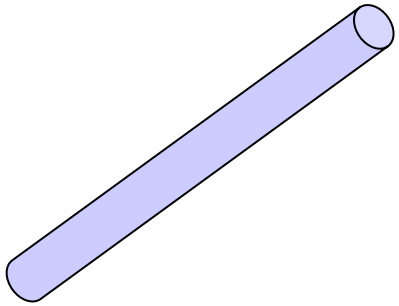

Segmented Nanowire (0D?)

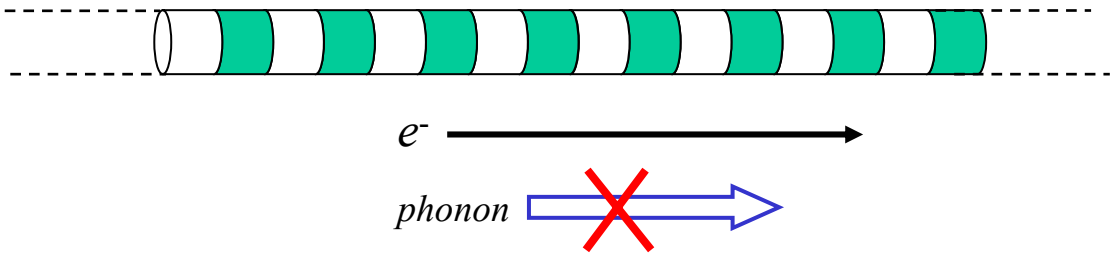

Segmented Nanowire Systems

2D + 1D = Better Thermoelectrics?

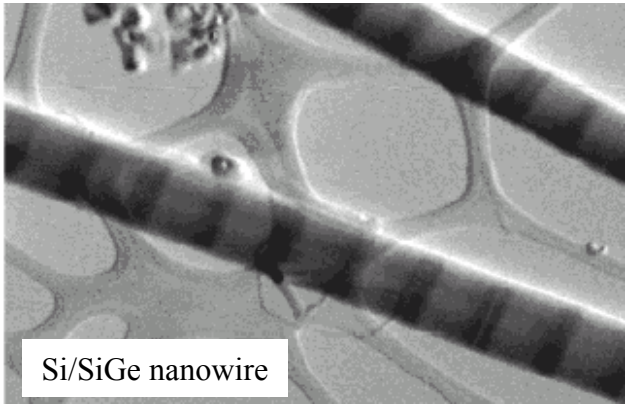

Wu *et al.*, Nano Letters (2002)

- Segmented Nanowires:
  - Superlattice in a 1D system
- Motivation
  - To take advantage of both the superlattices and the nanowires to design a better thermoelectric system
  - To substantially reduce the lattice thermal conductivity by increasing the phonon scattering at the segment interfaces
  - To gain insight and understanding of the enhanced thermopower S (and the power factor $S^2\sigma$) in quantum dot arrays *(Harman et al.)* and cross-plane superlattice systems *(Venkatasubramanian et al.)*
- In practice, segmented nanowires can be synthesized using a controlled electrochemical deposition system or laser-ablation approach *(Lieber et al, Samuelson et al., and Yang et al.)*

Enhancement in Seebeck Coefficient

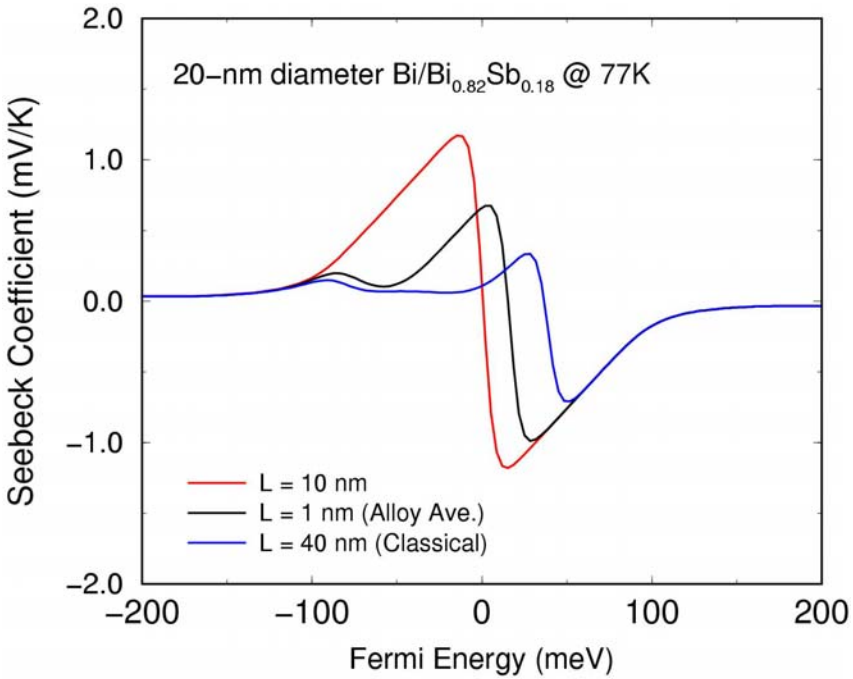

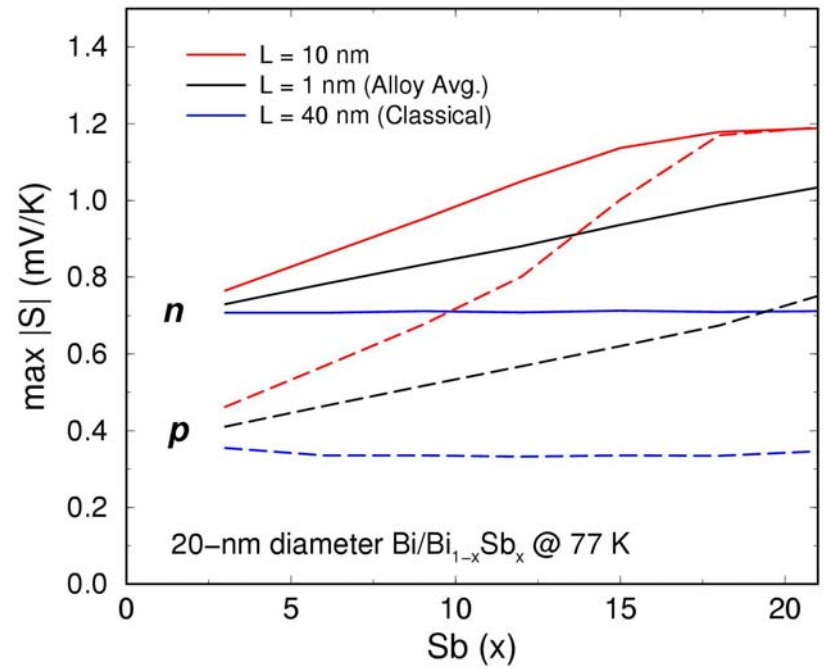

Calculated Seebeck coefficient of $Bi/Bi_{0.82}Sb_{0.18}$ segmented nanowires as a function of Fermi energy for different segment lengths at 77 K.

Maximal Seebeck coefficient of $Bi/Bi_{1-x}Sb_x$ segmented nanowires as a function of Sb content x for different segment lengths at 77 K.

Summary

- 2D
  - Proof of principle of enhanced *ZT*
  - Carrier pocket engineering concept applied
  - Experimental results show high *ZT* for cross-plane geometry
- 1D
  - Theoretically predicted enhancement of *ZT*
  - Experimental measurements verify theoretical model
- 0D
  - Experimental results of quantum dot superlattices show high *ZT*
  - Preliminary modeling results show enhanced Seebeck for segmented nanowires